Hypervelocity Stars*

Warren R. Brown

Smithsonian Astrophysical Observatory, Harvard-Smithsonian Center for Astrophysics, Cambridge, Massachusetts 02138; email: wbrown@cfa.harvard.edu

Annu. Rev. Astron. Astrophys. 2015. 53:15–49

First published online as a Review in Advance on April 15, 2015

The *Annual Review of Astronomy and Astrophysics* is online at astro.annualreviews.org

This article's doi:
10.1146/annurev-astro-082214-122230

Keywords

black holes, binary stars, stellar kinematics, stellar dynamics, Galactic Center, Galactic halo

Abstract

Hypervelocity stars (HVSs) travel with such extreme velocities that dynamical ejection via gravitational interaction with a massive black hole (MBH) is their most likely origin. Observers have discovered dozens of unbound main-sequence stars since the first in 2005, and the velocities, stellar nature, spatial distribution, and overall numbers of unbound B stars in the Milky Way halo all fit an MBH origin. Theorists have proposed various mechanisms for ejecting unbound stars, and these mechanisms can be tested with larger and more complete samples. HVSs' properties are linked to the nature and environment of the Milky Way's MBH, and, with future proper motion measurements, their trajectories may provide unique probes of the dark matter halo that surrounds the Milky Way.

1. INTRODUCTION

Hypervelocity stars (HVSs) are remarkable objects. HVSs are ejected by the Galaxy's central massive black hole (MBH) at speeds that exceed Galactic escape velocity. HVSs are now observed in the halo of the Milky Way. HVSs thus link the outer parts of the Milky Way to its very center and provide important tools for exploring a wide range of phenomena. The distribution of HVSs in space and velocity can reveal the existence of a binary MBH, for example. The stellar nature of HVSs is a probe of the mass function and binary population of the Galactic Center. The former companions of HVSs, stars that are bound in tight orbits around the MBH, become extreme mass ratio inspiral gravitational wave sources and tidal disruption events. HVSs may explain some hostless supernovae and isolated neutron stars. Finally, because an HVS integrates the gravitational pull of the Galaxy as it travels outward from the Galactic Center, the trajectories of HVSs provide unique and powerful probes of the shape and orientation of the Galaxy's dark matter halo.

Three-body exchange interactions among stars and an MBH inevitably unbind stars from a galaxy. Because stars have finite sizes, only a massive compact object can explain stars ejected at 1,000-km s^{-1} velocities. Hills (1988) predicted the existence of such unbound stars and called them hypervelocity stars. Hills followed his prediction with simulations to assess the ejection probabilities of HVSs as an observable test of MBHs (Hills 1991, 1992). A decade later, Yu & Tremaine (2003) proposed a binary MBH ejection scenario for HVSs and calculated rates for the single and binary MBH ejection scenarios. Despite the growing acceptance of MBHs in the centers of galaxies (Kormendy & Richstone 1995, Kormendy & Ho 2013), and thus the necessary existence of HVSs, these few papers [plus a work of science fiction: Paul McAuley (1991) used the idea of an HVS hurtling toward the Earth in his book *Eternal Light*] represent the entire interest in HVSs for 17 years.

The situation changed in 2005 with the discovery of the first HVS: a B-type star traveling out of the Galaxy with a velocity at least twice the Galactic escape velocity at its ~100-kpc distance (Brown et al. 2005). Strikingly, the star's present motion exceeds the escape velocity from the surface of the star. Such an extreme motion can be explained by neither supernova explosions in close binary systems (Blaauw 1961) nor dynamical encounters between binaries (Poveda et al. 1967), the mechanisms responsible for "runaway stars." To explain a motion in excess of the escape velocity from the surface of a star requires dynamical interaction with a massive compact object, as predicted by Hills (1988).

The discovery of the first observed HVS sparked a broad surge of interest in the concept of HVSs, a theoretical field that had lain dormant for nearly twenty years. When asked his opinion of the HVS discovery, Hills responded that it was "high time someone found it" (Perlman 2005). Hundreds of papers spanning a wide range of astronomy have since discussed HVSs now that observers have established their existence (**Figure 1**).

Since 2005 there have been many more HVS discoveries, both serendipitous and targeted. Follow-up observations have determined the stellar nature of these unbound stars, and the growing sample of unbound stars has revealed unexpected features in their spatial and velocity distributions. The existence of HVSs has inspired broad theoretical interest, and many testable predictions have emerged.

Physics provides many possible ways of accelerating stars to high velocities (e.g., Tutukov & Fedorova 2009), but the Hills mechanism is unique in its ability to eject large numbers of main-sequence stars at unbound velocities. Thus unbound main-sequence stars make the most compelling HVS candidates. HVSs can be ejected from any galaxy with an MBH; however, the intrinsic luminosity of stars limits observers' views to stars near the Milky Way. This review thus focuses on main-sequence HVSs in the Milky Way.

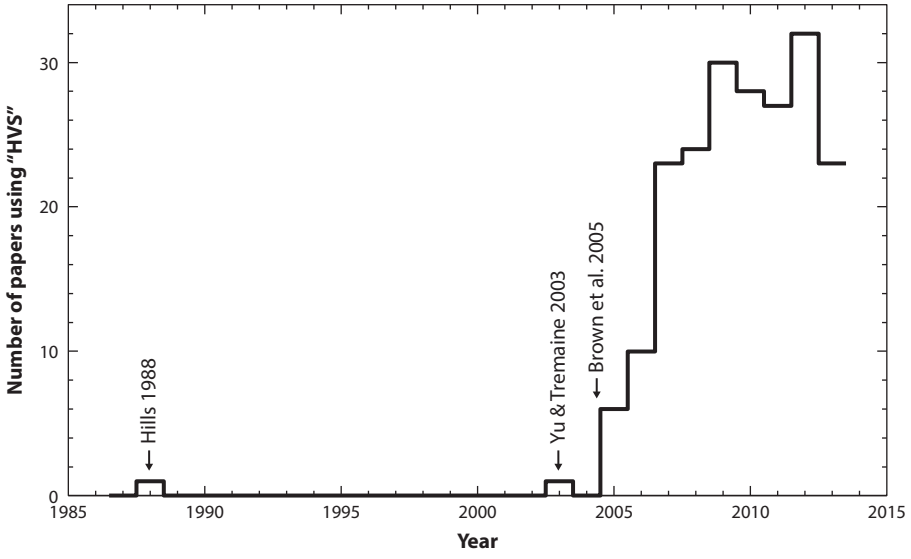

Figure 1

Number of refereed papers using the term "hypervelocity star" (HVS). The first HVS discovery by Brown et al. (2005) sparked a surge of interest in the concept of HVSs. (Data from ADS Labs full text search, vetted by eye.)

Identifying HVSs remains observationally difficult. The radial velocity of a main-sequence star is easily measured, for example, but its origin is not. Observers have instead obtained a wealth of indirect evidence, including the spatial distribution, velocity distribution, and flight time distribution of unbound HVSs, to support the HVS ejection scenario and rule out alternative scenarios.

To distinguish them from runaways and other phenomena, Hills coined the term HVS to describe a star ejected by a 3-body exchange with an MBH having a terminal velocity of $\sim$1,000 km s^{-1}. Two properties therefore define an HVS:

1. MBH ejection origin, and
2. Unbound velocity.

The first property is important, because not all unbound stars in the Milky Way are ejected by the MBH. HVSs exist together with normal Galactic stars. As we discuss further below, HVSs and disk runaways can have overlapping velocity distributions but have very different ejection mechanisms. We begin our discussion with the physics that underlies the HVS phenomena.

2. PHYSICAL UNDERSTANDING

The physical mechanism of the HVS ejection is a 3-body exchange involving an MBH. There are four major ingredients linking HVS theory to observations. The first ingredient is the multiplicity of stars, which opens the door to energy exchange scenarios. Second is the 3-body exchange with an MBH. Third is the Galactic gravitational potential, which modifies the motions of HVSs and acts as a high-pass filter on escaping stars. The final ingredient is the physical properties of the stars themselves, which modify the observed distribution of HVSs.

2.1. Multiplicity of Main-Sequence Stars

The majority of stars with mass $m_* > 1$ $M_\odot$ are in multiple, not single, systems, and this multiplicity is a function of stellar mass (Duchêne & Kraus 2013). Volume-limited surveys of stars within approximately 70 pc find that 46% of G-type stars are multiples (Tokovinin 2014), 60% of F-type stars are multiples (Fuhrmann & Chini 2012), and 70% of A-type stars are multiples (De Rosa et al. 2014). B- and O-type stars are rare and more difficult to constrain at large distances, but at least 50–80% of B- and O-type stars are multiples (Chini et al. 2012).

Massive stars occur more frequently in short orbital period systems. Half of binaries containing O-type stars have orbital periods less than 20 days. These O-type stars interact with their companions before ending their lives (Sana et al. 2012). Thus single O-type stars are, in many cases, the merger products of close binary systems (de Mink et al. 2014).

Observations also suggest that a nontrivial fraction of binaries are hierarchical triples or higher-order systems (Duchêne & Kraus 2013). Triple systems are stable when the semimajor axis of the tertiary is much larger than the semimajor axis of the inner binary (e.g., Perets 2009b). Because of their larger cross section, dynamical encounters with triples should dominate encounters in low- to moderate-density star clusters (Leigh & Geller 2013). Multiplicity, orbital period distributions, and their stellar mass dependence all have important consequences for the production of observable HVSs and the distribution of HVS ejection velocities.

2.2. Massive Black Holes

MBHs, black holes with masses $>10^5$ $M_\odot$, are believed to be ubiquitous in centers of galaxies (Kormendy & Ho 2013). The orbital motions of stars in the center of our Galaxy provide compelling evidence for a 4×10^6 $M_\odot$ MBH in the heart of the Milky Way (Ghez et al. 2008, Gillessen et al. 2009). The environments of these MBHs are characterized by extreme stellar densities, extreme velocities, and short dynamical timescales. Unusual dynamical phenomena are therefore frequent near an MBH.

An HVS is produced by a 3-body exchange between a stellar binary and an MBH (Hills 1988, 1991). An MBH tidally disrupts a stellar binary at the distance $r_{\rm bt}$ in which the MBH's gravitational tidal force exceeds the force that binds the binary,

$$r_{\rm bt} = a\left(\frac{3M}{m_{\rm b}}\right)^{1/3} \simeq 14\ {\rm AU}\left(\frac{a}{0.1\ {\rm AU}}\right)\left(\frac{{\rm M}_\odot}{m_{\rm b}}\right)^{1/3}\left(\frac{M}{10^6\ {\rm M}_\odot}\right)^{1/3}. \quad (1)$$

Here, a is the semimajor axis of the binary, $m_{\rm b}$ is the total mass of the binary, and M is the MBH mass (Miller et al. 2005).

Energy conservation demands that a 3-body exchange with an MBH ejects an HVS. **Figure 2** illustrates the interaction. For a 4×10^6-$M_\odot$ MBH, the orbital velocity at the binary tidal disruption distance is $v = \sqrt{GM/r_{\rm bt}} \simeq 10{,}000$ km s^{-1}, which is a few percent of the speed of light. Such velocities are observed in the Galactic Center (Ghez et al. 2005). For comparison, the orbital velocity of stars in an equal mass binary is $v_{\rm b} = \sqrt{Gm_{\rm b}/a} = 94$ km s$^{-1}\sqrt{(m_{\rm b}/{\rm M}_\odot)(0.1\ {\rm AU}/a)}$, or 100 km s^{-1} for a pair of 3-$M_\odot$ stars in an $a = 0.5$-AU binary. At the moment of tidal disruption by the MBH, the stars have a relative motion of order $v_{\rm b}$ and thus experience a change in specific energy $\delta E = 1/2(v+v_{\rm b})^2 - 1/2v^2 \simeq vv_{\rm b}$ (Hills 1988, Yu & Tremaine 2003). To conserve energy, the ejected star has a final velocity at infinite distance from the MBH of $v_{\rm ej} = \sqrt{2vv_{\rm b}} \simeq 1{,}000$ km s^{-1}.

Numerical simulations predict the distribution of HVS ejection velocities in greater detail. Both the HVS ejection velocity and the probability of ejection are linked to the semimajor axis of the stellar binary. Compact binaries are disrupted less frequently but yield higher ejection velocities.

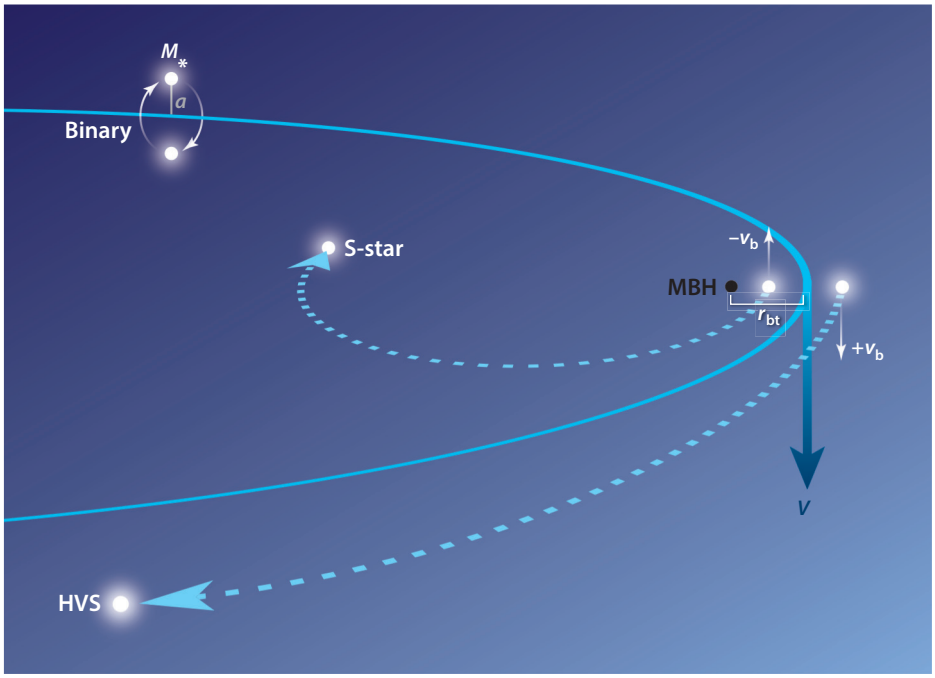

Figure 2

Schematic illustration of the Hills mechanism, a 3-body exchange in which a massive black hole (MBH) replaces one component of a stellar binary and ejects a hypervelocity star (HVS). Here, a binary star of mass m_b, semimajor axis a, and orbital velocity v_b drops toward an MBH of mass M. The velocity v at pericenter is orders of magnitude larger than v_b. If the pericenter distance is less than the binary tidal disruption distance r_{bt}, the binary is disrupted: One star becomes gravitationally bound to the MBH and, by conservation of energy, the other star is ejected at approximately the geometric mean of v and v_b. Figure inspired by J. Guillochon.

HVSs ejected by a 3-body exchange with an MBH have a final velocity at infinite distance from the MBH,

$$v_{ej} = 1{,}370 \text{ km s}^{-1} \left(\frac{a}{0.1 \text{ AU}}\right)^{-1/2} \left(\frac{m_b}{M_\odot}\right)^{1/3} \left(\frac{M}{4 \times 10^6 M_\odot}\right)^{1/6} f_R, \quad (2)$$

where f_R is a factor of order unity that depends on r_{peri}, the periapse distance to the MBH (Hills 1988, Bromley et al. 2006, Kenyon et al. 2008). The probability of an ejection also depends on the periapse distance to the MBH. Given the dimensionless quantity defined by Hills (1988),

$$D = \left(\frac{r_{peri}}{a}\right) \left(\frac{10^6}{M} \frac{m_b}{2}\right)^{1/3}, \quad (3)$$

the probability of an ejection P_{ej} is

$$P_{ej} \simeq 1 - D/175 \quad (4)$$

for $0 \leq D \leq 175$ (Hills 1988, Bromley et al. 2006). For $D > 175$, the binary does not approach close enough to the MBH to produce an ejection.

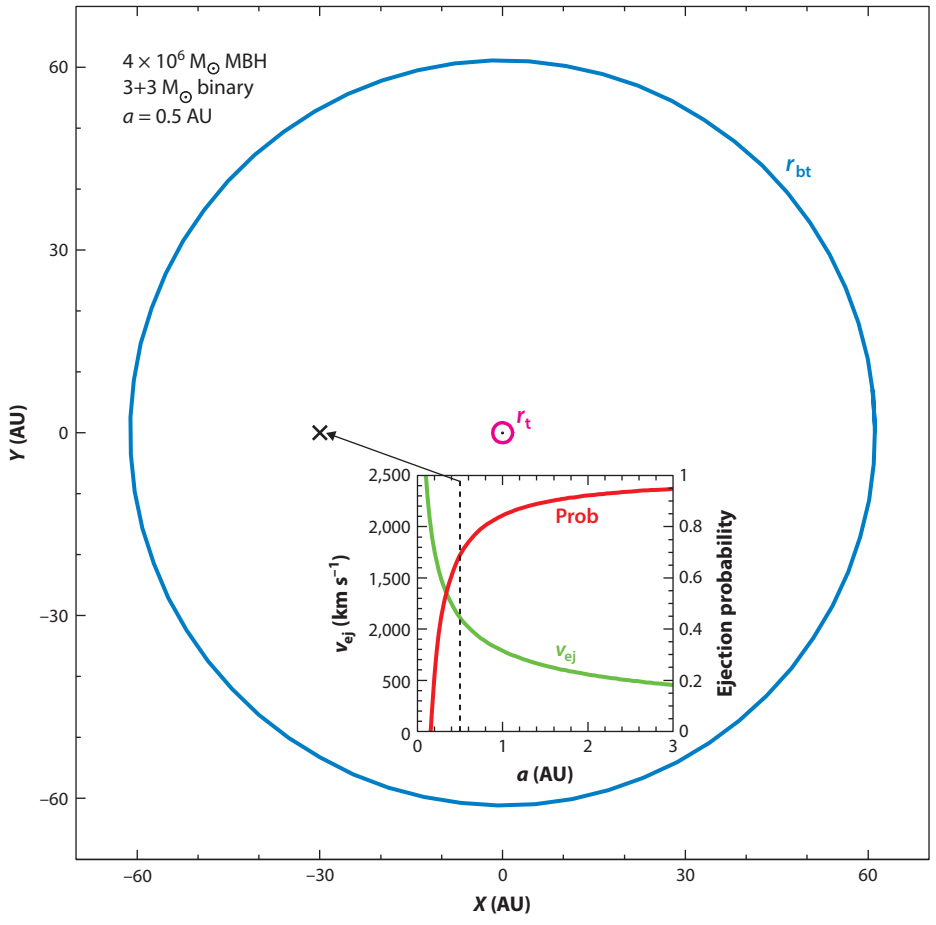

Figure 3

Binary tidal disruption radius r_{bt} (*blue circle*) compared with the stellar tidal disruption radius r_t (*magenta circle*) for a 4×10^6 $M_\odot$ massive black hole (MBH) and a $3 + 3$ $M_\odot$ binary with $a = 0.5$ AU. The black dot at the center is the Schwarzschild radius of the MBH approximately to scale. The inset shows the predicted 1,000 km s^{-1} hypervelocity star (HVS) ejection velocity (*green line*) and 75% probability of ejection (*red line*) for a 30-AU periapse distance (indicated by the ×).

Figure 3 illustrates these quantities for a 4×10^6-$M_\odot$ MBH and a fiducial $3 + 3$-$M_\odot$ binary with $a = 0.5$ AU. The binary tidal disruption distance r_{bt} is approximately 36 times larger than the tidal disruption radius of the individual 3-$M_\odot$ stars (see below). The inset of **Figure 3** shows the predicted HVS ejection velocity and the probability of ejection as functions of the binary semimajor axis for a 30-AU periapse distance.

Whether a stellar binary is disrupted or continues to orbit the MBH or whether its members collide depends on the details of the encounter, such as the orbital phase of the binary at the moment of tidal disruption. Stars that end up colliding with a relative velocity less than stellar escape velocity result in a merger; the merger product is bound to the MBH (Ginsburg & Loeb 2006, 2007). Collisions among binary members most likely occur after multiple orbits around the MBH. HVS ejections are produced primarily during a binary's first $r_{peri} < r_{bt}$ passage around the MBH (Antonini et al. 2010, 2011).

2.3. Variations on a Massive Black Hole

Variations on the Hills mechanism include 3-body interactions with a binary MBH (Yu & Tremaine 2003) and 3-body interactions with stellar mass black holes (SBHs) orbiting the central MBH (O'Leary & Loeb 2008). Stars stripped from a tidally disrupting dwarf galaxy passing through the Galactic Center are another proposed mechanism (Abadi et al. 2009). A final possibility is a supersonic gas cloud, launched from an active galactic nucleus (AGN), that collapses to form HVSs (Silk et al. 2012).

Binary MBHs are an expected consequence of galaxy mergers. Three-body interactions with a binary MBH can eject single stars as HVSs (Yu & Tremaine 2003). In this scenario, the most energetic ejections occur in the direction of MBH orbital motion. A circular binary MBH preferentially ejects HVSs from the orbital plane of the binary MBH; an eccentric binary MBH ejects HVSs in a broad jet. Ejections become more energetic and isotropic as the binary MBH hardens and then merges on 1–10-Myr timescales (Gualandris et al. 2005; Baumgardt et al. 2006; Levin 2006; Sesana et al. 2006, 2008). An observational signature of a binary MBH in-spiral event is thus a distinctive burst of HVSs in a ring or shell. The binary MBH scenario differs from the Hills mechanism in that the ejection velocity of HVSs does not depend on the mass of the stars. In fact, a binary MBH can eject binary stars (Lu et al. 2007).

Binary HVSs may not be unique to binary MBHs, however. Encounters between hierarchical triples and a single MBH can disrupt the outer star and eject the inner binary as a binary HVS (Perets 2009b). Simulations suggest that, in both scenarios, HVS binaries constitute a few percent of all HVS ejections (Lu et al. 2007, Perets 2009b, Sesana et al. 2009).

A variant of the binary MBH is a 10^3–10^4-$M_\odot$ intermediate mass black hole (IMBH)-MBH binary. Observations of our Galactic Center exclude an equal mass binary MBH but cannot exclude an IMBH orbiting the MBH (Reid & Brunthaler 2004). Three-body interactions with an IMBH-MBH binary can naturally eject HVSs. If star formation is ongoing in the Galactic Center, and if IMBHs are formed by collisional runaway of stars in massive young star clusters near the central MBH, then IMBH-MBH in-spiral events may generate periodic bursts of HVSs every $\sim 10^7$ years (Portegies Zwart et al. 2006). The cored distribution of old stars surrounding the Milky Way's central MBH is perhaps a signature of a past IMBH in-spiral event (Baumgardt et al. 2006).

Another mechanism for ejecting HVSs is the 3-body interaction between a single star and an SBH orbiting an MBH (O'Leary & Loeb 2008). SBHs are the remnants of massive stars that should migrate, by dynamical friction, into the region surrounding the central MBH (Morris 1993). HVS ejections occur if the SBHs form a cusp and are fed by a relaxed distribution of stars (O'Leary & Loeb 2008). The SBH scenario differs from the Hills mechanism in two notable respects. First, SBH encounters are unlikely to generate ejection velocities exceeding 1,000 km s^{-1}. Second, SBH encounters eject the lowest-mass stars with the highest ejection velocities.

A tidally disrupting dwarf galaxy on a close pericenter passage can also eject stars (Abadi et al. 2009), though a massive $>10^{10}$-$M_\odot$ dwarf galaxy is necessary to eject unbound stars (Piffl et al. 2011). The signature of the tidal debris scenario is a clump of unbound stars of all stellar types connected to a stream of bound stars.

As an alternative to these stellar dynamical mechanisms, theorists propose that HVSs may be explained by stars formed inside gas clouds launched from an AGN jet (Silk et al. 2012) or AGN spherical outflow (Zubovas et al. 2013). The challenge in this picture is whether a supersonic gas cloud collapses to form stars. Observed star formation occurs in clumps and cores inside subsonic giant molecular clouds (McKee & Ostriker 2007). The uncertain physics of the AGN scenario has precluded any predictions of HVS velocities or ejection rates. If AGN-ejected gas clouds collapse to form stars, this scenario implies that HVSs should be found in discrete clumps with common velocities.

2.4. Galactic Potential

Regardless of exact origin, HVSs are decelerated by the gravitational pull of the Galaxy's extended mass distribution as they escape the Milky Way. To understand the motion of HVSs therefore requires a Galaxy model that accurately reproduces the gravitational potential from the very center out to the outer halo. Historically, potential models for the Milky Way developed for other applications were optimized to fit observations at distances $R > 200$ pc from the Galactic Center, in which R is the radial distance from the Galactic Center. However, for HVSs the largest deceleration occurs at $R < 200$ pc. To address this problem, Kenyon et al. (2008) derive a three-component bulge-disk-halo potential model that fits observed mass measurements from the Galactic Center to the outer halo. The model was originally designed for a 220-km s^{-1} circular velocity. Updating the Kenyon et al. (2008) disk mass $M_d = 6 \times 10^{10}$ $M_\odot$ and disk radial scale length $a_d = 2.75$ kpc yields a flat rotation curve of 235 km s^{-1} consistent with the most recent circular velocity measurements (Reid et al. 2014).

Figure 4 illustrates the radial acceleration profile of the Galaxy, decomposed into the contributions from the central MBH, bulge, disk, and halo for the updated Kenyon et al. (2008) model. The acceleration and velocity profiles are calculated along the z-axis of the axisymmetric model. Profiles calculated along the Galactic plane are 2% higher. The important point is that the highest acceleration occurs in the inner 100 pc of the Milky Way. The gravitational potential of the inner Galaxy thus acts as a high-pass filter, allowing only high-velocity ejections to reach the outer parts of the Galaxy.

Figure 4*b* plots the radial velocity profiles for stars dropped from different starting distances in this model. The MBH radius of influence, the distance at which its gravitational acceleration equals that of the surrounding stars, is a couple of parsecs. For a star starting at $R = 1$ pc, **Figure 4** shows that the star must move at >700 km s^{-1} to reach the solar circle at $R = 8$ kpc, >800 km s^{-1} to reach the edge of the disk at $R = 25$ kpc, and >900 km s^{-1} to reach the virial radius at $R = 250$ kpc.

The velocity profile that extends to the virial radius provides an estimate of Galactic escape velocity for this potential model. At the Solar circle $R = 8$ kpc, the effective escape velocity is 578 km s^{-1}, consistent with current Solar Neighborhood escape velocity measurements (Smith et al. 2007, Piffl et al. 2014). At $R = 50$ kpc in the halo, the escape velocity is 367 km s^{-1}. Clearly, no one velocity threshold can define an unbound star; whether a star of a given speed is unbound or not depends on its location in the Milky Way.

2.5. Physical Properties of Stars

Stars have three fundamental properties that affect the detection of HVSs: their physical size, intrinsic luminosity, and finite lifetime, all of which are related to stellar mass. We discuss each property in turn.

The physical size of stars imposes a speed limit on ejection velocity. For stellar encounters with an MBH, the speed limit is set by the tidal disruption distance of a star by the MBH:

$$r_t = \left(\frac{M}{m_*}\right)^{1/3} r_* \simeq 0.5 \text{ AU} \left(\frac{M}{10^6\, m_*}\right)^{1/3} \frac{r_*}{R_\odot}, \quad (5)$$

where M is the mass of the MBH, m_* is the mass of the star, and r_* is the radius of the star. The fastest HVSs come from the closest encounters with an MBH, but stars passing closer than r_t produce tidal disruption events, not HVSs. The Schwarzschild radius, for comparison, has a linear dependence on black hole mass, $r_{MBH} = 2GM/c^2 = 0.02$ AU$(M/10^6$ $M_\odot)$, where G is the

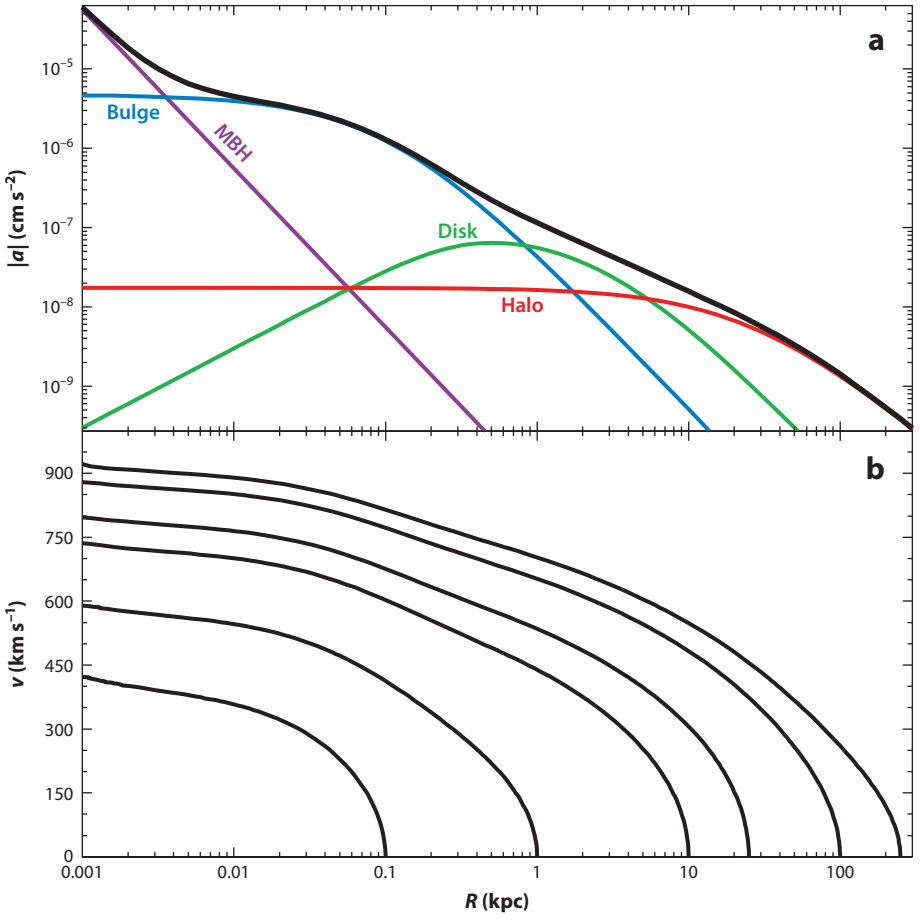

Figure 4

(*a*) Radial acceleration in the Galactic potential, decomposed into contributions from the central massive black hole (MBH; *purple line*), bulge (*blue line*), disk (*green line*), and halo (*red line*). The black line is the total acceleration. Acceleration and velocity profiles are calculated along the *z*-axis for convenience; profiles calculated along the Galactic plane differ by 2% in this model. (*b*) The radial velocity profile of stars dropped from different radial starting locations (*black lines*). The velocity profile from the virial radius $R = 250$ kpc provides an estimate of Galactic escape velocity in this model. Adapted from Kenyon et al. (2008) with permission.

gravitational constant and c is the speed of light. The stellar tidal disruption distance is less than the Schwarzschild radius when the MBH mass exceeds approximately 10^8 $M_\odot$ (Hills 1975). In other words, main-sequence stars fall through the MBH event horizon before tidal disruption for $M > 10^8$ $M_\odot$.

For stellar encounters between individual stars, the speed limit of an ejection is set by the escape velocity from the surface of a star. To achieve higher speeds, stars would have to orbit inside each other, which is physically impossible. The escape velocity from the surface of a star is

$$v_{esc*} = \left(\frac{2Gm_*}{r_*}\right)^{1/2} = 618\left(\frac{m_*}{M_\odot}\frac{R_\odot}{r_*}\right)^{1/2} \text{km s}^{-1}. \quad (6)$$

Because of the quasi-linear relationship between the mass and radius of main-sequence stars, $v_{esc*} \simeq 600$ km s^{-1} to within 10% for 0.4–4-$M_\odot$ main-sequence stars. Stellar encounters between individual stars cannot produce speeds in excess of this velocity (Leonard 1991).

HVSs are a natural explanation for main-sequence stars ejected at speeds greater than v_{esc*}. The typical $v_{ej} \simeq 1{,}370$-km s^{-1} ejection velocity of the Hills mechanism (Equation 2) significantly exceeds the v_{esc*} of a typical main-sequence star (Equation 6). Compact stellar remnants, such as neutron stars, have larger escape velocities and can attain higher ejection velocities. However, neutron stars are the product of supernova explosions, and all high-velocity neutron stars observed to date can be explained with natal kicks (Hansen & Phinney 1997, Chatterjee et al. 2005).

The intrinsic luminosity of stars determines the survey volume accessible for a given stellar type of HVS. Magnitude-limited surveys that reach to twentieth magnitude, such as the Sloan Digital Sky Survey (SDSS) and *Gaia*, can sample solar metallicity 0.5-$M_\odot$ stars to heliocentric distance $d = 1$ kpc, 1-$M_\odot$ stars to $d = 10$ kpc, and 3-$M_\odot$ stars to $d = 100$ kpc (e.g., Girardi et al. 2004). Metal-poor stars are systematically less luminous for the same effective temperature and thus probe smaller volumes.

The finite lifetimes of stars dictate what types of HVSs are observed and where. In 1 Myr, a star moving at 1,000 km s^{-1} travels 1 kpc. Thus short-lived O-type HVSs do not live long enough to travel out of the Galactic bulge. Long-lived HVSs can cross megaparsec distances. Long-lived stars exist in every part of the Milky Way, which makes distinguishing long-lived HVSs from normal Milky Way stars difficult. However, HVSs with short lifetimes can only originate from regions of ongoing star formation, such as the Galactic disk and Galactic Center.

Finally, stellar lifetime also affects the observed velocity distribution of HVSs. A star dropped from rest at the virial radius of the Milky Way reaches the Galactic Center in approximately 1 Gyr. That means stars with <1-Gyr lifetimes ejected from the Galaxy on marginally bound orbits cannot be observed on inbound trajectories, as they do not live long enough to return. By contrast, stars with >1-Gyr lifetimes can fully populate bound orbits. Bound ejections accumulate and dominate the population of long-lived stars at all distances in the Galaxy (Kenyon et al. 2008). This has important implications for the most likely contaminant in HVS surveys: runaway stars.

3. POINT OF CONFUSION: RUNAWAY STARS

Runaways, historically defined in the context of O and B stars, are Galactic disk stars with peculiar motions faster than 40 km s^{-1} (Blaauw 1961). Silva & Napiwotzki (2011) provide an excellent recent discussion of runaways.

Runaways were initially identified by Humason & Zwicky (1947) as B-type stars at unexpectedly large distances from the disk. Greenstein & Sargent (1974) establish that these B-type stars are a mix of objects: some are evolved stars that belong in the halo, but many are main-sequence B stars, short-lived stars that began their lives in the disk. In the Solar Neighborhood, approximately 30% of O-type stars and 10% of B-type stars are runaways based on their peculiar velocities (Gies & Bolton 1986, Stone 1991). All runaway B stars in the Solar Neighborhood have orbits consistent with a disk origin (Martin 2006). Solar Neighborhood runaways also have a multiplicity many times lower than that of disk O and B stars (Gies & Bolton 1986). Because most O and B stars are born as binaries, runaways are naturally explained by binary disruption mechanisms. There are two proposed ejection mechanisms: supernova ejections and dynamical ejections.

In the supernova ejection mechanism, a runaway is released from a binary when its former companion explodes as a supernova (Blaauw 1961). The maximum possible ejection velocity in the supernova mechanism is the sum of the supernova kick velocity and the orbital velocity of the progenitor binary, or 200–300 km s^{-1} (Portegies Zwart 2000). Velocities up to 400 km s^{-1} may

be possible for binaries containing an early B and a Wolf-Rayet star (Przybilla et al. 2008a). Most ejections occur with much lower velocity and in all cases are below Galactic escape velocity.

In the dynamical ejection mechanism, a runaway is ejected by dynamical 3- or 4-body interactions in a young star cluster (Poveda et al. 1967). The maximum possible ejection velocity in the dynamical ejection mechanism is set by the escape velocity of the most massive star (Leonard 1991). Ejection velocities can reach 500–600 km s^{-1} for 4-$M_\odot$ stars interacting with contact binaries containing 100-$M_\odot$ stars (Gvaramadze et al. 2009, Gvaramadze & Gualandris 2011). However, smoothed particle hydrodynamic simulations of stellar binary-binary interactions find that high-velocity encounters frequently yield merger events instead of ejections owing to tidal dissipation effects (Fregeau et al. 2004). Recent simulations predict that the velocities from dynamical ejection form a power-law distribution; 99% of dynamical ejections have <200-km s^{-1} velocities (Perets & Subr 2012).

Observations demonstrate that both the supernova and dynamical ejection mechanisms occur in nature (Hoogerwerf et al. 2001). A runaway can possibly experience both a dynamical and a supernova ejection in a two-step process, but this phenomenon should apply to only ∼1% of O-type runaways (Pflamm-Altenburg & Kroupa 2010). The most important observation in the context of HVSs is the discovery by Heber et al. (2008a) of the first hyper-runaway B star, an unbound runaway star that was ejected from the outer disk.

Observations place only limited constraints on the overall velocity and spatial distribution of runaways in the Galaxy. Magnitude-limited surveys, such as the Hipparcos sample (Martin 2004, 2006), are complete in volumes centered on the Solar Neighborhood. Simulations predict that the overall distribution of runaways in the Galaxy reflects their origin from the rotating disk. Runaways ejected from the Galactic disk naturally have a flattened spatial distribution with a scale height comparable to the thick disk. The kinematics of runaways also reflect their disk origin: The fastest runaways are those ejected at the lowest Galactic latitudes in the direction of rotation (Bromley et al. 2009).

3.1. Runaway Ejection Rates

To understand whether runaways may be confused with HVSs requires that we know their ejection rates as well as their spatial and velocity distributions. If we assume that (*a*) the Milky Way forms stars at 1 $M_\odot$ $year^{-1}$ (Robitaille & Whitney 2010), (*b*) the stars have a Kroupa mass function ranging from 0.08 to 100 $M_\odot$ (Weidner & Kroupa 2006), and (*c*) 0.1% of stars become runaways (Silva & Napiwotzki 2011), then runaways are launched from the disk at a rate of 2×10^{-3} $year^{-1}$. Because most runaway ejections are bound, we expect that runaways dominate the population of velocity outliers near the disk.

3.2. Hyper-Runaway Ejection Rates

In the halo, runaways that move at >400 km s^{-1} at $R = 50$ kpc are the only ones that can be confused with HVSs. Such hyper-runaways are rare. To have a 400-km s^{-1} velocity at $R = 50$ kpc requires a 600-km s^{-1} ejection from the Solar circle. A 600-km s^{-1} runaway can be explained only by the dynamical ejection mechanism. The rate of 600-km s^{-1} ejections is related to the joint probability of interacting contact binaries containing very massive stars within the lifetimes of the very massive stars. Quantitatively, the Perets & Subr (2012) dynamical ejection velocity model predicts that 4×10^{-4} of runaways are ejected at ≥600 km s^{-1}. The ejection rate of hyper-runaways with speeds comparable with HVSs is thus 8×10^{-7} $year^{-1}$. For context, this hyper-runway rate is approximately 1% of the HVS ejection rate (see below).

Galactic rotation and outer disk launch locations can reduce the velocity required to create a hyper-runaway; however, neither effect increases the overall ejection rate. If runaway ejections are randomly oriented, for example, 10% of runaways experience a $\geq$200-km s^{-1} boost from being ejected in the direction of Galactic rotation. This boost reduces the required ejection velocity from 600 km s^{-1} to 400 km s^{-1} at the Solar circle. The fraction of hyper-runaways remains approximately 10^{-4}, however, because 2×10^{-3} of runaways are ejected with velocities $\geq$400 km s^{-1} (Perets & Subr 2012) and 10% are ejected in the direction of rotation. Launching runaways from the outer disk, $R = 20$–25 kpc, reduces the required ejection velocity from 600 km s^{-1} to 500 km s^{-1}. However, the outer disk is 6–8 exponential scale lengths removed from the Solar circle (Porcel et al. 1998, Bovy & Rix 2013) and thus contains 1,000 times fewer stars than the region of the Solar circle. Combined with the dynamical ejection velocity distribution, 100 times fewer hyper-runaways are launched from the outer disk than from the Solar circle. Accounting for all these effects simultaneously, models predict that there should be approximately 1 hyper-runaway per 100 HVSs in the halo (Bromley et al. 2009, Perets & Subr 2012, Kenyon et al. 2014).

4. HVS EJECTION RATES

HVSs are an inevitable consequence of MBHs in the centers of galaxies, but the number of HVSs that can be observed depends on the ejection rate of HVSs. HVSs are most easily observed in the Milky Way. We therefore begin by describing the environment of the MBH in our Galactic Center and the observational constraints on binaries in the Galactic Center. We then discuss the dynamical processes that scatter these stars onto orbits that encounter the MBH (the "loss cone"). We conclude with an estimate of the Milky Way HVS ejection rate and a discussion of its observational consequences.

4.1. Massive Black Hole Environment: The Galactic Center

The center of the Milky Way presents the best-studied picture of an MBH and its environment. The 4×10^6-$M_\odot$ MBH sits at the dynamical center of the Milky Way (Reid & Brunthaler 2004) surrounded by an immense crowd of stars. Within 1 arcsec = 0.04 pc of the MBH, several dozen main-sequence B-type stars (the so-called S stars) move on randomly oriented, eccentric orbits around the MBH (Ghez et al. 2008, Gillessen et al. 2009). The relative absence of evolved giant stars in the central few arcseconds suggests the MBH sits in a cored distribution of stars, not a relaxed cusp (Buchholz et al. 2009; Do et al. 2009, 2013; Bartko et al. 2010).

Slightly further out, over 100 very young O-type stars exist between 1 arcsec and 12 arcsec from the MBH. Half of these O stars orbit together in a clockwise thin disk (Levin & Beloborodov 2003; Bartko et al. 2009, 2010; Lu et al. 2009; Yelda et al. 2014). This young stellar disk appears to have an unusual top-heavy stellar mass function (Nayakshin & Sunyaev 2005, Bartko et al. 2010, Lu et al. 2013), consistent with in situ formation scenarios in a former massive gas disk (Levin & Beloborodov 2003, Nayakshin 2006).

Spectroscopic analysis of the other stars in the central 1 pc indicates that the central region has experienced continuous but variable star formation over the past 12 Gyr (Pfuhl et al. 2011). Surrounding the young stellar disk, but on a different orbital plane, is a 10^6-$M_\odot$ circumnuclear torus of molecular gas 2–8 pc from the MBH (Guesten et al. 1987, Christopher et al. 2005). A nuclear star cluster, composed mostly of old stars with a half-light radius of 4.2 pc and a mass of 2.5×10^7 $M_\odot$ (Schodel et al. 2014), envelops the entire central region.

At 30-pc projected distances from the MBH are the Arches and Quintuplet clusters, two of the most massive young star clusters in the Milky Way (Figer et al. 1999). Clearly, there is no lack of stars that form and orbit near the Milky Way's central MBH.

4.2. Binaries in the Galactic Center

Two spectroscopic binaries (Pfuhl et al. 2014) and one eclipsing binary (Ott et al. 1999) are observed among the massive O stars near the MBH. These detections imply that the binary fraction of massive O stars near the MBH is comparable with the fraction observed in nearby dense star clusters. There are also four transient X-ray sources in the central 1 pc that can be interpreted either as low-mass X-ray binaries, possibly the product of 3-body encounters between binaries and stellar remnants, or as high-mass X-ray binaries associated with the young stellar disk (Muno et al. 2005).

Theoretically, the binary fraction of stars in the Galactic Center is expected to evolve as a result of dynamical interactions. In the environment near the MBH, most binaries appear soft and will eventually be disrupted by encounters with other stars. The disruption timescale for an $a = 1.0$-AU binary, $R = 1$ pc from the MBH, is $\sim 10^8$ years (Perets 2009a). Long-lived stars should have a very low binary fraction near the MBH. Thus low-mass binaries that encounter the MBH must come from beyond $R > 1$ pc (Hopman 2009). Massive OB stars, in contrast, have lifetimes less than the binary disruption time; encounters between massive binaries and the MBH are limited primarily by stellar evolution.

Not all binary encounters with the MBH necessarily make HVSs. Wide binaries are easily disrupted, but their disruption yields low ejection velocities (Equation 2). Compact binaries, by contrast, have a lower probability of disruption (Equation 4) but are more frequent than wide binaries. There is more energy in a compact binary. Thus the disruption of compact binaries yields the highest ejection velocities. Binaries with $a < 1$ AU are the most likely sources of unbound HVSs (**Figure 3**), and they are also the most likely to survive in the Galactic Center.

4.3. Massive Black Hole Loss Cone

The rate at which stars encounter the MBH depends on the timescale for scattering stars into the MBH "loss cone." The loss cone is the phase space of low angular momentum orbits that have close periapse distances to the MBH. Assuming that stars on loss cone orbits are rapidly eliminated, the steady-state encounter rate of stars with the MBH is controlled by dynamical processes that refill the "empty loss cone." This process is complex because different dynamical processes operate on different timescales and spatial scales in the Galactic Center. Two-body relaxation is one of the dominant dynamical processes. Because binaries have larger tidal radii than single stars, the empty loss cone regime for MBH–stellar binary interactions can extend out to large, >100 pc, distances from the MBH.

Theoretical calculations traditionally assume that the MBH sits in a relaxed spherical cusp (Bahcall & Wolf 1976). In the spherical equilibrium assumption, there is a well-defined rate at which 2-body gravitational encounters between stars fill the loss cone (Merritt 2013). There is, however, both observational (Buchholz et al. 2009, Do et al. 2013) and theoretical (Antonini 2014) evidence that the Milky Way has a core and thus an unrelaxed stellar distribution. Furthermore, observations show that the distribution of mass in the Galactic Center is not spherical but triaxial (Stolte et al. 2008). Torquing of orbits by a triaxial potential causes much higher encounter rates than in a spherical potential. A triaxial potential also contains orbits that encounter the MBH at any finite time (Merritt 2013). Thus the assumption of a spherical, empty loss cone is very likely wrong, but its 2-body relaxation timescale remains a useful point of reference.

Two-body gravitational encounters with massive objects, such as giant molecular clouds, greatly increase the rate of stellar encounters with the MBH (Perets et al. 2007). Although the number density of "massive perturbers" is small compared with the density of stars, these objects are so much more massive than stars that they dominate the gravitational scattering inside any region that

contains them. In the Milky Way, massive perturbers dominate 2-body relaxation timescales at 100-pc distances. Perets et al. (2007) estimate that the observed distribution of massive perturbers in the Galactic Center enhances the MBH encounter rate of stellar binaries by a factor of 10–1,000 compared with spherical equilibrium 2-body relaxation.

Binaries formed in a former gaseous disk around the MBH may also add to the MBH encounter rate. Binaries embedded in a massive gas disk migrate toward the MBH as in planetary migration scenarios (Levin 2007, Baruteau et al. 2011). The presence of a massive gas disk also acts to enlarge the MBH loss cone (Karas & Subr 2007).

In the absence of gas, the orbits of stars in a young stellar disk evolve owing to resonant relaxation on timescales shorter than 2-body relaxation (Rauch & Tremaine 1996). A cusp of SBHs further enhances the evolution of orbital eccentricities and thus the encounter rate of disk stars with the MBH (Löckmann et al. 2009; Madigan et al. 2009, 2011). A cusp of 1,000 SBHs within 0.1 pc can produce the observed distribution of S stars in theoretical models (Antonini 2014). A cusp may not be required if the stellar disk was once more massive and extended closer to the MBH; in that case, the disk itself could rapidly evolve the orbital eccentricities of the innermost disk stars (Chen & Amaro-Seoane 2014).

Another possible process for quickly moving stars into the MBH loss cone is the in-spiral of a massive star cluster hosting an IMBH. The in-spiral of a massive star cluster was originally proposed to explain the short-lived S stars orbiting the MBH (Gerhard 2001), but it was later realized that any star cluster would be tidally destroyed before reaching the MBH unless it hosts an IMBH (Hansen & Milosavljević 2003). Models of a massive star cluster+IMBH in-spiral can explain the observed distribution of S stars (Merritt et al. 2009) but overpredict the number of short-lived stars outside the central 1-pc region (Perets & Gualandris 2010).

The Galactic Center clearly hosts a wealth of dynamical processes that cause binaries to encounter the MBH. The binary encounter rate depends in part on where the binaries originate, but all the dynamical processes mentioned here act to increase the encounter rate over the spherical equilibrium, 2-body relaxation rate. HVS ejection probabilities and ejection velocities ultimately depend on how binaries encounter the MBH (Bromley et al. 2006, Zhang et al. 2010, Kobayashi et al. 2012).

4.4. Milky Way HVS Ejection Rate

Hills (1988) estimates a theoretical Milky Way HVS ejection rate of 10^{-3}–10^{-4} year^{-1}. This estimate is based on the number of hard $a = 0.1$–1-AU binaries expected to encounter the MBH in a full loss cone. Yu & Tremaine (2003) affirm this estimate but argue that the MBH loss cone should be empty. For an empty loss cone fed at the 2-body relaxation rate, the Milky Way HVS ejection rate is 10^{-5}–10^{-6} year^{-1}. A single MBH in the Galactic Center cannot produce fewer HVSs than this empty loss cone rate. We note that massive perturbers alone increase the empty loss cone rate by a factor of 100 (Perets et al. 2007), bringing the Yu & Tremaine (2003) rate up to the full loss cone rate estimated by Hills (1988).

Zhang et al. (2013) provide the most sophisticated HVS ejection rate calculation to date. They consider models that inject binaries both from stellar disks and from infinity, which is appropriate for the massive perturber model. Zhang et al. (2013) also consider different stellar mass functions to compare the models with the observed S stars in the Galactic Center and the B-type HVSs in the Galactic halo. The models that best match the set of observations have HVS ejection rates of 10^{-4}–10^{-5} year^{-1}.

Theoretical HVS ejection rate estimates are also available for binary MBH scenarios. In a spherical galaxy at equilibrium, a pair of MBHs stalls at 1-pc separation and ejects HVSs at a

rate of 10^{-4} year^{-1} (Yu & Tremaine 2003). For the case of an in-spiraling IMBH-MBH binary, models predict comparable $\sim 10^{-4}$ year^{-1} HVS ejection rates over the 1–10 Myr in-spiral time of the IMBH (Sesana et al. 2008, Gualandris & Merritt 2009).

We adopt 10^{-4} year^{-1} as the likely Milky Way HVS ejection rate given the various theoretical results. Tidal disruption events provide a consistency check. Tidal disruption events require closer encounters with an MBH than the HVS scenario (see **Figure 3**) and thus should have comparable or lower rates. Indeed, the rate of observed tidal disruption events in nearby galaxies is 10 times lower than the adopted Milky Way HVS ejection rate (Donley et al. 2002, Wang & Merritt 2004, Gezari et al. 2009, van Velzen & Farrar 2014).

Notably, the 10^{-4} year^{-1} Milky Way HVS ejection rate is 100 times larger than the ejection rate of disk runaways with speeds comparable with HVSs. Thus contamination of HVS surveys with runaways should be negligible.

4.5. Observational Consequences

A rate of 10^{-4} year^{-1} means that HVSs are rare. The rarity of HVSs has observational consequences. For example, to detect a rare object in a rare phase of its lifetime is unlikely. Stars spend most of their lifetimes on the main sequence.

If HVS ejections are continuous and isotropic, the density of HVSs goes approximately as r^{-2}:

$$\rho(r) = \frac{\mathrm{d}N/\mathrm{d}t}{4\pi r^2 \mathrm{d}r/\mathrm{d}t} \simeq \frac{100\,\mathrm{Myr}^{-1}}{4\pi r^2 (1{,}000\ \mathrm{km\,s}^{-1})} = \frac{8}{r^2}\mathrm{kpc}^{-3}. \quad (7)$$

Thus, assuming a fiducial speed of 1,000 km s^{-1} = 1 kpc Myr^{-1}, the nearest HVS of any type is 1 kpc from the Sun. The rarity of HVSs means that even the nearest HVS is unlikely to have a large proper motion.

Finding more than one HVS requires sampling large volumes of space. Within 10 kpc of the MBH there are of order 10^3 HVSs and 10^{11} Milky Way stars, a contrast ratio of $1{:}10^8$. The outer halo of the Milky Way, by comparison, contains far fewer stars and has a density profile that declines more steeply than r^{-2} (Deason et al. 2014). These facts explain why most unbound HVSs observed to date are found in the halo and why they are primarily identified by radial velocity.

5. A BRIEF HISTORY OF HVS AND CANDIDATE HVS OBSERVATIONS

We now provide a brief history of HVS observations. Candidate HVSs have been identified in different ways over time, first by radial velocity and more recently by tangential velocity. Not all candidate HVSs are likely to be HVSs.

The first HVS, hereinafter HVS1, was discovered serendipitously in a radial velocity survey of faint blue horizontal branch stars in the outer halo (Brown et al. 2005). **Figure 5** presents the observation. HVS1's heliocentric radial velocity $+831 \pm 6$ km s^{-1} corresponds to a velocity of at least 673 km s^{-1} in the Galactic rest frame (Brown et al. 2014). Time-series photometry reveals that HVS1 is a slowly pulsating B star (Fuentes et al. 2006), although this is disputed (Turner et al. 2009). Spectroscopic stellar atmosphere model fits by two different groups show that HVS1 has $v \sin i \simeq 190$ km s^{-1} and thus is a relatively short-lived 3-$M_\odot$ main-sequence star based on its rapid rotation (Heber et al. 2008b, Brown et al. 2014). HVS1 is a compelling HVS candidate because its motion significantly exceeds the escape velocity from the surface of the star.

After the discovery of HVS1, two other serendipitous HVS discoveries were published. The next is a helium-rich subdwarf O star, US708, traveling with a velocity of at least 720 km s^{-1} in the Galactic rest frame (Hirsch et al. 2005). US708 can be thought of as a proto-white dwarf, a

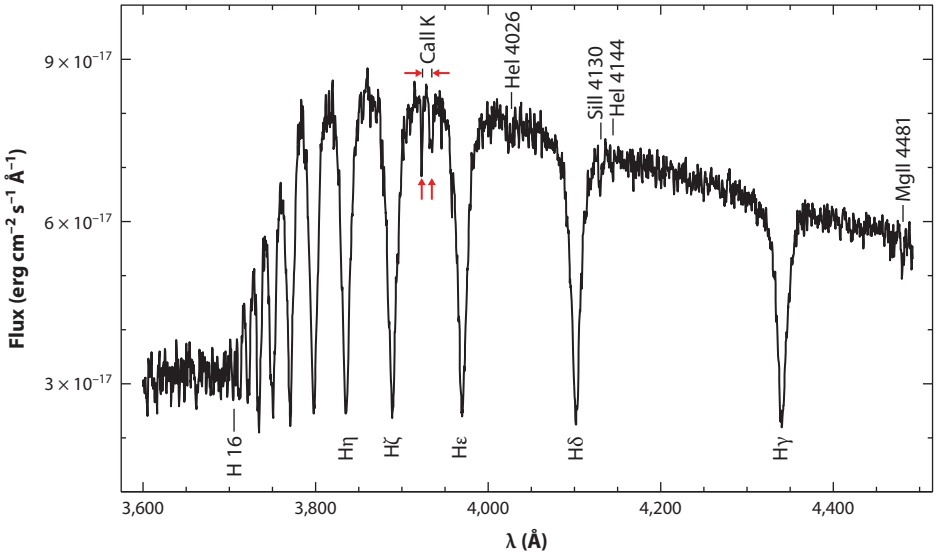

Figure 5

Spectrum of HVS1, shifted to rest frame. Hydrogen Balmer lines dominate the spectrum; this is a B9 star with $T_{\rm eff} = 11{,}200$ K and $\log g = 3.8$ (Brown et al. 2014). The 11-Å separation between the two CaII K lines (*red arrows*), the narrow line from the local interstellar medium, and the broad line from the atmosphere of the star, visibly show the star's +831 km s^{-1} heliocentric radial velocity.

hot but intrinsically faint star without detectable hydrogen. The evolutionary history of He-sdO stars is unclear, but one possibility consistent with subdwarf studies is that they are the merger products of two He-core white dwarfs (Hirsch et al. 2005). Justham et al. (2009) and Wang & Han (2009) propose an alternative theory: a helium star kicked at a velocity >400 km s^{-1} by a Type Ia supernovae explosion from a single-degenerate white dwarf+helium star binary (see also Geier et al. 2013, Wang et al. 2013). If the supernova scenario is correct, US708 can originate from anywhere in the Milky Way. US708 is close enough that future proper motion measurements should discriminate between HVS and Type Ia supernova origins.

The third early HVS discovery, HE 0437–5439 (Edelmann et al. 2005), is moving with a velocity of at least 530 km s^{-1} in the Galactic rest frame. This star is intriguing for at least two reasons. First, HE 0437−5439 is only 16° away from the Large Magellanic Cloud (LMC). Second, stellar atmosphere fits identify HE 0437−5439 as a 9-$M_\odot$ main-sequence star 50 kpc away (Bonanos et al. 2008, Przybilla et al. 2008b). The lifetime of this star is many times shorter than its flight time from the Milky Way, suggesting an LMC origin. However, an LMC origin requires a 1,000-km s^{-1} ejection and thus an unseen MBH or IMBH in the LMC (Edelmann et al. 2005, Gualandris & Portegies Zwart 2007). A Milky Way origin, by contrast, requires a blue straggler origin for HE 0437−5439. In other words, the progenitor was a binary system ejected from the Milky Way at >800 km s^{-1}. Two proposed mechanisms for accomplishing this feat are a binary MBH that ejects stellar binaries as HVSs (Lu et al. 2007) and a single MBH that ejects binaries by triple disruption (Perets 2009b). Initial proper motion measurements indicate that HE 0437−5439 is moving away from the Milky Way (Brown et al. 2010).

These serendipitous HVS discoveries motivated the targeted HVS Survey by Brown et al. (2006a,b, 2007a,b, 2009a, 2012b, 2014). The HVS Survey is a well-defined spectroscopic survey of stars with the colors of $\simeq$3-$M_\odot$ stars. These stars should not be found at faint magnitudes in the

outer halo unless they were ejected there. The HVS Survey is complete over 12,000 deg^2 (29%) of sky and identifies 21 significantly unbound stars in radial velocity alone. Correcting for stellar lifetime, these discoveries imply that unbound 2.5–4-$M_\odot$ stars are ejected from the Milky Way at a rate of 1.5×10^{-6} year^{-1}. The HVS Survey also identifies a comparable number of bound velocity outliers with +300-km s^{-1} speeds in the outer halo. The absence of −300-km s^{-1} stars in the HVS Survey demonstrates that the observed +300-km s^{-1} stars have lifetimes less than 1 Gyr; they are probably $\simeq$ 3-$M_\odot$ stars ejected on bound trajectories.

Radial velocity surveys have not yet uncovered lower-mass HVSs, a fact that reflects the space density of low-mass HVSs. Kunder et al. (2012) report a radial velocity outlier in their survey of bulge M giants, but the star is probably bound. Kollmeier et al. (2009, 2010) search the SDSS spectroscopic catalog for unbound F-type stars and find none. The absence of unbound F-type stars implies that the mass function of HVS progenitors is top-heavy or else the mechanism for ejecting HVSs favors massive stars. Both conclusions are consistent with the Hills mechanism and Galactic Center observations.

A different approach for finding unbound stars combines radial velocity and proper motion. The most important discovery is HD 271791, an 11-$M_\odot$ B star that is 21 kpc distant from the Sun and moving with a velocity of at least 600 km s^{-1} in the Galactic rest frame (Heber et al. 2008a). HD 271791 is significantly unbound. Its measured proper motion points not from the Galactic Center, however, but from the outer disk. HD 271791 is thus the first example of an unbound runaway star, or hyper-runaway, ejected in the direction of rotation from the outer disk by stellar binary disruption processes (Przybilla et al. 2008a, Gvaramadze et al. 2009).

A similar object was recently announced by the LAMOST spectroscopic survey (Zheng et al. 2014). LAMOST-HVS1 is a 9-$M_\odot$ B star that is 13 kpc distant from the Sun and moving with a velocity of at least 477 km s^{-1} in the Galactic rest frame. The star is marginally unbound in radial velocity. The star can come from either the Galactic disk or the Galactic Center, depending on what proper motion measurement is adopted.

There are a wide variety of other candidate HVSs identified primarily by tangential velocity. These tangential velocity outliers include a 2.5-$M_\odot$ A star (Tillich et al. 2009), a 5-$M_\odot$ B star (Irrgang et al. 2010), an evolved sdB star (Tillich et al. 2011), some metal-poor F stars (Li et al. 2012), a metal-poor CH giant star (Pereira et al. 2012), two red horizontal branch stars (Pereira et al. 2013), nearby G and K stars (Palladino et al. 2014), and a mix of nearby stars from LAMOST (Zhong et al. 2014).

The difficulty in understanding these diverse tangential velocity outliers lies in evaluating the accuracy of their proper motion and distance estimates. Proper motion systematic errors are rarely taken into account. Distance uncertainties can be a factor of 2 even in well-studied cases (Pereira et al. 2013). False-positives are problematic because proper motions cannot be easily checked given the required time baseline for their measurement. If one takes published error bars at face value, those HVS candidates unbound at >1-σ confidence are the sdB star J1211+1437 (Tillich et al. 2011), the metal-poor F star J2218−0040 (Li et al. 2012), the A/F stars J085819.9+150352 and J092707.0+242753 (Zhong et al. 2014), and perhaps a dozen of the G and K dwarfs (Palladino et al. 2014). All these objects are near the Galactic disk. The metallicities of the G and K dwarfs match a disk population, and their trajectories come from the disk. The observations suggest that many of the tangential velocity outliers are probably disk runaways.

6. THE PRESENT OBSERVATIONAL UNDERSTANDING OF HVSs

Comparing observations to theory can constrain the origin of HVSs. Different HVS ejection mechanisms predict different ejection velocity distributions, spatial distributions, and ejection

rates. No observation to date directly links an unbound star to the MBH; however, there are many observations that provide indirect evidence for HVSs. The best evidence comes from the properties of the unbound stars in the halo: their velocities, stellar nature, flight times, ages, angular positions, and overall numbers. In addition, the existence of HVSs requires that their former companions still orbit the MBH. The stellar nature and orbital distribution of the S stars are well explained by the HVS ejection scenario.

In this section we step through each observational constraint. Although individual observations can be explained in different ways, only the HVS mechanism can self-consistently explain all the observations together.

6.1. Velocity Distribution of HVSs

6.1.1. Background. Extreme velocity is a fundamental characteristic of HVSs. However, extreme velocity is not a sufficient criterion for identifying HVSs, because an MBH is not the only possible source of unbound stars.

Because HVSs are launched on radial trajectories from the Galactic Center, spectroscopic radial velocities measure the major component of motion for all but the very nearest HVSs. Measurement uncertainty depends on details like spectral resolution and the spectral type of the star, but typical radial velocity errors are 1–10 km s^{-1} or 0.1–1% of HVS motion. Tangential velocity can be measured for nearby ($\leq$10 kpc) distances. Measurement uncertainty depends on both proper motion errors and distance errors, however. At the >1-kpc distances of the nearest HVSs, typical tangential velocity errors are 10–100 km s^{-1} or 1–10% of HVS motion. Radial velocity therefore provides the most accurate constraint on motion.

Velocity distribution provides a second constraint. All MBH ejection mechanisms produce a spectrum of ejection velocities (e.g., Bromley et al. 2006). A binary MBH launches more >1,000 km s^{-1} HVSs than a single MBH, for example. With a sample of 100 HVSs, the distribution of HVS velocities can distinguish the two MBH mechanisms (Sesana et al. 2007). The necessary existence of bound ejections can also be used as a discriminant. For short-lived stars, there should be comparable numbers of bound and unbound HVSs on outbound trajectories in the halo, along with an absence of bound stars on inbound trajectories (Kenyon et al. 2008).

6.1.2. Observations. To study the observed velocity distribution of HVSs, we turn to the HVS Survey by Brown et al. (2014). The HVS Survey is a well-defined spectroscopic survey of halo stars complete over 12,000 deg^2 of sky. Importantly, the HVS Survey selects for B-type stars by broadband color only; no kinematic selection effect is imposed on the sample.

The HVS Survey identifies 21 unbound late B-type stars in the halo. These 21 B-type stars are significantly unbound in radial velocity alone. The unbound stars are all moving outward, which is consistent with an ejection from the Galactic Center. No inward moving stars with comparable velocity are found in the HVS Survey.

The fastest unbound stars in the HVS Survey have 700-km s^{-1} speeds at distances of 50–100 kpc. A speed of 700 km s^{-1} significantly exceeds their stellar escape velocity and provides strong evidence for an MBH ejection scenario. The present lack of a >1,000-km s^{-1} star is in slight tension with HVS ejection models (Sesana et al. 2007, Kenyon et al. 2008, Zhang et al. 2013, Rossi et al. 2014); however, the overall distribution of radial velocity and distance is consistent with HVS ejection models (Kenyon et al. 2014).

The HVS Survey also contains a significant excess of bound +300-km s^{-1} velocity outliers. The absence of a comparable number of −300-km s^{-1} stars in the HVS Survey demonstrates that most of the +300-km s^{-1} stars have lifetimes less than their $\simeq$1 Gyr orbital turnaround time

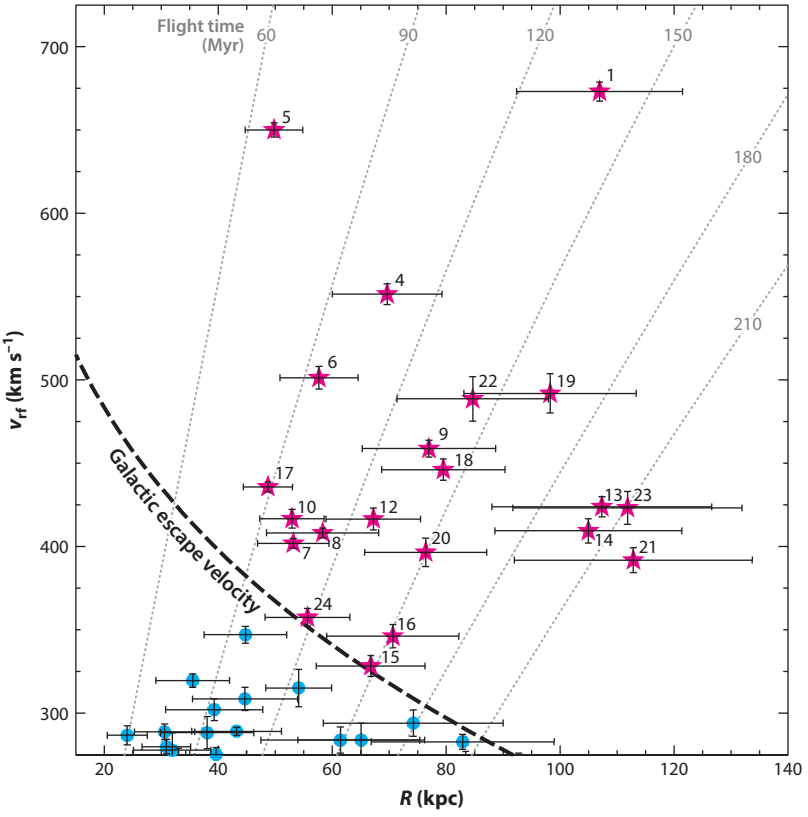

Figure 6

Observed Galactic rest frame velocity v_{rf} and Galactocentric distance R of late B-type stars in the Hypervelocity Star (HVS) Survey. The dashed line is the Galactic escape velocity from the updated Kenyon et al. (2008) model (**Figure 4**). Dotted gray lines are isochrones of flight time from the Galactic Center. Unbound HVSs are marked by magenta stars; possible bound HVSs are marked by blue circles. Adapted from Brown et al. (2014) with permission.

(Brown et al. 2007b, Kollmeier & Gould 2007, Yu & Madau 2007). In other words, the bound outliers in the HVS Survey are short-lived B stars at 50–100-kpc distances. The MBH ejection scenario requires the existence of bound ejections, and the observed unbound and bound velocity outliers in the HVS Survey fit the MBH ejection picture (**Figure 6**).

6.2. Metallicity

6.2.1. Background. Metallicity provides a possible constraint on the origin of HVSs. If HVSs are short-lived stars, their abundance patterns should reflect their place of origin.

Stars formed in the Galactic Center are expected to have solar iron abundance and possibly enhanced alpha element abundance (Carr et al. 2000, Ramírez et al. 2000, Ryde & Schultheis 2015). Stars formed in the Galactic disk should have [M/H] $= +0.3$ if they originate from $R =$ 4 kpc and [M/H] $= -0.4$ if they originate from $R = 14$ kpc (Hayden et al. 2014). Early B-type stars in the Solar Neighborhood have solar abundance [M/H] $= 0.0$ (Nieva & Przybilla 2012). If HVSs are the tidal debris of a typical star-forming dwarf galaxy in the Local Group, the stars should have $-2 <$ [M/H] < -0.5 (McConnachie 2012).

Unfortunately, metallicity does not always reflect place of origin. There is observational (Gebran et al. 2010) and theoretical (Hopkins 2014) evidence that stars within a single cluster have a statistically significant spread in abundances. Furthermore, hot stars with radiative atmospheres are frequently observed with peculiar abundance patterns. Gravitational settling and radiative levitation of elements in the atmospheres of these stars systematically change their surface abundances over time (Michaud 1970, Bailey et al. 2014). In other words, the surface abundance pattern of B-type HVSs may no longer reflect their original composition.

Stellar rotation also puts a practical limitation on metallicity measurements. Young stars are fast rotators. Fast rotation smears weak metal lines and makes accurate abundance measurements difficult.

6.2.2. Observations. High spectral resolution echelle observations are available for the 9-$M_\odot$ unbound B star near the LMC, HE 0437−5439 (Edelmann et al. 2005, Bonanos et al. 2008, Przybilla et al. 2008b) and for the four brightest unbound B stars in the HVS Survey, HVS5 (Brown et al. 2012a), HVS7 (López-Morales & Bonanos 2008, Przybilla et al. 2008c), HVS8 (López-Morales & Bonanos 2008), and HVS17 (Brown et al. 2013).

HE 0437−5439, HVS7, and HVS17 have solar iron abundances but a wide scatter in other elemental abundances. The subsolar C, N, Mg, and Si abundances of HE 0437−5439 are consistent with either an outer Galactic disk or LMC origin for that star (Przybilla et al. 2008b). HVS7 and HVS17, by contrast, are identified as Bp stars. Sophisticated, non-local thermodynamic equilibrium modeling of the atmosphere of HVS7 finds underabundant He and C, 10 times overabundant iron group elements, and 10,000 times overabundant rare-earth elements and Hg (Przybilla et al. 2008c). The peculiar abundance pattern of HVS7 provides no meaningful constraint on its origin. HVS5 and HVS8 rotate too rapidly for metal line measurements. We conclude that present abundance measurements of HVSs provide no meaningful constraint on their origin.

6.3. Stellar Rotation

6.3.1. Background. Projected stellar rotation, $v \sin i$, constrains the origin of HVSs in two ways. First, $v \sin i$ is the least ambiguous measure of the stellar nature of B spectral-type stars. B-type main-sequence stars and evolved horizontal branch stars can have similar effective temperatures and surface gravities but very different rotations. Main-sequence B stars are young and have mean $v \sin i \simeq 150$ km s^{-1} (Abt et al. 2002, Huang & Gies 2006). Hot horizontal branch stars are old stars that have evolved off the giant branch and have $v \sin i < 7$ km s^{-1} (Behr 2003a,b). Fast rotation is thus the clear signature of a young main-sequence star.

Second, the distribution of $v \sin i$ may be linked to the nature of the HVS ejection mechanism. If HVSs are the product of disrupted compact binaries, then the mean $v \sin i$ of late B-type HVSs should be relatively slow, $v \sin i \simeq 70$ km s^{-1}, because of the tidal synchronization of the progenitor binaries (Hansen 2007). The binary MBH ejection mechanism, in contrast, can eject single fast-rotating stars and may even spin-up stars during the ejection (Löckmann & Baumgardt 2008). However, to be significantly spun-up, an HVS must deeply penetrate its stellar tidal disruption radius (Antonini et al. 2011).

6.3.2. Observations. The five unbound B stars with echelle spectroscopy are fast rotators with $55 < v \sin i < 260$ km s^{-1}. All five stars are thus short-lived main-sequence B stars based on their rotation. Even the slowest rotating object spins 10 times faster than the fastest rotating evolved star of the same temperature.

The moderate spectral resolution observations of the other unbound stars in the HVS Survey can identify objects with very rapid rotation. In the HVS Survey, there are six unbound B stars

that have 200–300-km s^{-1} rotation and six unbound B stars with marginally significant rotation around 170 km s^{-1} (Heber et al. 2008b, Brown et al. 2014). Altogether, approximately half of the unbound B-type stars in the HVS Survey are firmly identified as short-lived main-sequence stars on the basis of rotation. These unbound B stars, currently located at $R = 50$–100 kpc in the halo, must originate from a region with recent star formation.

Present measurements do not significantly constrain the distribution of $v \sin i$. The five unbound B stars with echelle spectroscopy have a mean $v \sin i = 114$ km s^{-1} and a dispersion on the mean of ± 39 km s^{-1}. These five HVSs thus appear equally likely to be drawn from a population of single main-sequence stars with mean $v \sin i = 150$ km s^{-1} or a population of (disrupted) tidally synchronized binaries with mean $v \sin i = 70$ km s^{-1}.

6.4. Flight Time

6.4.1. Background. The distribution of HVS flight times is another constraint on HVS origin. A burst of HVSs is expected for an IMBH-MBH inspiral event, for example, or for a dwarf galaxy tidal disruption scenario (Abadi et al. 2009). If HVSs are ejected in bursts, both long-lived and short-lived HVSs must share a common flight time. By contrast, a continuous distribution of HVS flight times is consistent with the single MBH ejection scenario.

Flight time also provides a consistency check on the stellar nature of HVSs. We refer to the main-sequence lifetime of a star as the total amount of time it can spend on the main sequence. HVSs cannot be normal main-sequence stars if they have flight times longer than their main-sequence star lifetimes.

6.4.2. Observations. The distribution of flight times for the unbound stars in the HVS Survey is best described by a continuous ejection process (Brown et al. 2014). However, the uncertainties are large, and one cannot rule out that half of the unbound stars were ejected in a single burst. Multiple bursts would be required to explain the full span of observed flight times (see **Figure 6**).

In all cases, the unbound stars in the HVS Survey have flight times less than the main-sequence lifetimes of B stars, which is consistent with their identification as main-sequence stars ejected from the Milky Way. The 9-$M_\odot$ B star near the LMC is different (Edelmann et al. 2005). The flight time of HE 0437−5439 from the Galactic Center is 100 Myr, approximately 5 times longer than its $\simeq$20 Myr main-sequence lifetime (Przybilla et al. 2008b). The only way to reconcile the main-sequence nature of HE 0437−5439 with a Galactic origin is to identify it as a blue straggler, the stellar evolutionary product of two stars. Alternatively, an LMC origin solves the flight time problem but requires that HE 0437−5439 was ejected at a velocity of 1,000 km s^{-1} from the LMC. Neither explanation appears likely. Additional constraints are needed for this object.

6.5. Stellar Age and Arrival Time

6.5.1. Background. The time between the formation and ejection of an HVS provides a strong test of origin. We refer to the difference between formation and ejection as the "arrival time," because this is the time it takes the progenitor to arrive at the MBH in the Hills scenario (Brown et al. 2012a). Arrival time is a useful discriminant because high-velocity runaway ejections require massive stars, stars that have $\simeq 10^7$-year lifetimes. The arrival time of unbound runaway ejections is therefore $\leq 10^7$ years. Binaries formed in the Galactic Center, in contrast, should enter the MBH loss cone on timescales of 10^8–10^9 years (Yu & Tremaine 2003, Merritt & Poon 2004, Wang & Merritt 2004, Perets et al. 2007). There is no upper limit on arrival time in the MBH scenario, because an MBH can eject HVSs at any time.

6.5.2. Observations. To estimate arrival time, we subtract an HVS's age from its flight time from the Galaxy. Age is determined by comparing a star's surface gravity and effective temperature against stellar evolution models. Statistically meaningful age estimates can only be obtained from high signal-to-noise, high-resolution spectroscopy. HE 0437−5439 was the first well-studied unbound B star, but it remains a special case as discussed above (Edelmann et al. 2005, Przybilla et al. 2008b). The four brightest unbound B stars in the HVS Survey are 3.7−3.9-$M_\odot$ main-sequence B stars that have 63–105-Myr arrival times (Brown et al. 2012a, 2013). Typical arrival time uncertainties are $\pm 30\%$. Thus for the four unbound B stars in the HVS Survey, ejection during the first 10 Myr of their lifetimes is ruled out at the 2–3-σ level. In other words, the arrival times of these four unbound B stars are fully consistent with a Galactic Center origin but difficult to reconcile with any mechanism that requires prompt ejection.

The hyper-runaway discovered by Heber et al. (2008a) provides an interesting comparison. The proper motion of the hyper-runaway points to an origin from the outer disk. The star's 25 ± 5-Myr age and 25 ± 6-Myr flight time from the disk yield an arrival time of 0 ± 8 Myr, which is consistent with its disk runaway origin.

6.6. Number and Rate of Unbound HVSs

6.6.1. Background. Ejection rates provide a fundamental connection between observation and theory. Different ejection mechanisms produce different ejection rates of unbound stars. Thus the observed number of unbound stars provides a constraint on their origin.

Comparing different types of stars is difficult because of the unknown stellar mass function, multiplicity, and orbital distribution of HVS progenitors. Here, we consider the ejection rate of specific types of stars targeted in well-defined surveys.

6.6.2. Observations. We begin with the 20 G- and K-type stars with possible unbound tangential velocity (Palladino et al. 2014). These stars are drawn from the SDSS+SEGUE spectroscopic catalog, which has a 1,500 deg^2 (3.6% of sky) footprint. In that footprint, the SEGUE spectroscopic stars represent $\simeq$5% of the number count of G- and K-type stars as defined by the SEGUE color/magnitude cuts (Yanny et al. 2009). The tangential velocity outliers have heliocentric distances ranging from 1 to 6 kpc and thus probe a 33-kpc^3 volume in that footprint. Putting these numbers together yields a density of $\simeq$12-kpc^{-3} unbound G- and K-type stars near the Sun. If the observed tangential velocities map onto purely radial trajectories, the ejection rate of unbound G- and K-type stars is $\sim 10^{-2}$ $year^{-1}$ (Equation 7). The G- and K-type stars with unbound tangential velocities are thus much more numerous than any runaway or HVS ejection mechanism can explain.

A search through 291,111 SDSS stellar spectra finds zero G- and F-type stars with unbound radial velocity (Kollmeier et al. 2009). A careful consideration of survey volume yields an upper limit on the ejection rate of unbound G-type stars of $<3 \times 10^{-4}$ $year^{-1}$. An optimized search for unbound F-type stars in the SDSS+SEGUE also yields a null detection and provides a similar upper limit on the ejection rate of unbound F-type stars of $<4 \times 10^{-4}$ $year^{-1}$ (Kollmeier et al. 2010). Compared with the number of unbound B-type stars, these limits imply that HVSs do not have a Salpeter mass function. Alternatively, these limits imply that the HVS ejection mechanism favors high-mass stars. These conclusions are consistent with the stellar mass dependence of binary star properties and the Hills ejection scenario.

SDSS has also obtained spectra for over 10,000 A-type stars, approximately half of which are evolved blue horizontal branch stars visible out to 60-kpc distances (Sirko et al. 2004, Xue et al. 2011). Only one of these stars is claimed to be an unbound HVS (Brown et al. 2009a). This star is

one of the bluest and faintest stars in the SDSS horizontal branch sample, and its identification as an evolved blue horizontal branch star is ambiguous (Xue et al. 2011). A meaningful ejection rate estimate is therefore not possible.

The HVS Survey, by comparison, finds 21 unbound late B-type stars in a complete radial velocity survey that covers 12,000 deg^2 or 29% of sky (Brown et al. 2014). The unbound stars are identified as 2.5–4-$M_\odot$ main-sequence stars at 50–120 kpc distances on the basis of their fast rotation. The finite lifetimes of the B stars mean that a third of them should be absent at 50 kpc, and two-thirds should be absent at 100 kpc. Accounting for stellar lifetime, the observations imply there are $\simeq$300 unbound 2.5-4-$M_\odot$ HVSs over the entire sky within $R < 100$ kpc. The ejection rate of unbound 2.5–4-$M_\odot$ stars is thus 1.5×10^{-6} year^{-1}. Because 2.5–4-$M_\odot$ stars represent 1% of the stellar mass function by number, the observed rate of unbound late B-type stars is consistent with the theoretical 10^{-4} year^{-1} HVS ejection rate but is 100 times greater than the hyper-runaway rate. The number of unbound B stars in the halo therefore supports a Galactic Center origin.

6.7. Spatial Distribution

6.7.1. Background. The spatial distribution of HVSs—whether they are found in a clump, in a ring, or in a more isotropic distribution—provides another constraint on their origin. Alternative explanations for HVSs, such as dwarf galaxy tidal debris or disk runaway ejections, require distinctive distributions of unbound stars on the sky. An MBH, by contrast, can in principle eject an HVS in any direction. **Figure 7** illustrates possible spatial distributions.

Disk runaways can be launched in any direction, but the fastest runaways are those ejected in the direction of Galactic rotation. Simulations predict that 90% of hyper-runaways are to be found at Galactic latitudes $b < 25°$ (Bromley et al. 2009). The signature of hyper-runaways is thus a flattened spatial distribution of unbound stars with all possible flight times, reflecting an origin from the rotating disk.

A clump of unbound stars may be explained as the tidal debris of a dwarf galaxy that experienced a very close pericenter passage to the Milky Way (Abadi et al. 2009). Massive ($>10^{10}$ $M_\odot$) dwarf galaxies are the most likely progenitors of such unbound stars (Piffl et al. 2011). The signature of the tidal debris scenario is a clump of unbound stars that share a common flight time.

In the binary MBH ejection scenario, the highest-velocity ejections occur from the MBH orbital plane. An eccentric binary MBH may produce a jet of HVSs (Levin 2006, Sesana et al. 2006). As the binary MBH hardens, its orbital plane is perturbed on rapid timescales, and HVS ejections should become more energetic and isotropic (Gualandris et al. 2005, Baumgardt et al. 2006, Levin 2006, Sesana et al. 2006, 2008). Thus the signature of the binary MBH in-spiral scenario may be a ring, jet, or shell of HVSs with similar flight times.

In the single MBH ejection scenario, the direction of HVS ejection corresponds to the direction that the progenitor encounters the MBH. If HVS progenitors come from a dynamically relaxed population of stars in the Galactic Center, the spatial distribution of HVS ejections should be isotropic. If HVS progenitors come from a stellar disk, the spatial distribution of HVSs should lie on a plane (Lu et al. 2010; Zhang et al. 2010, 2013).

Even if HVSs are ejected isotropically, a nonspherical Galactic potential can modify the observed distribution of HVSs (Kenyon et al. 2008, Brown et al. 2009b). Stars ejected along the major axis of a potential are decelerated less at a given distance than those ejected along the minor axis. An initially isotropic distribution of HVSs ejected near escape velocity can thus appear anisotropic to an observer looking for HVSs in the halo. The predicted spatial distribution depends on the axis ratio and the rotation direction of the potential. If there is rotation around the long axis of

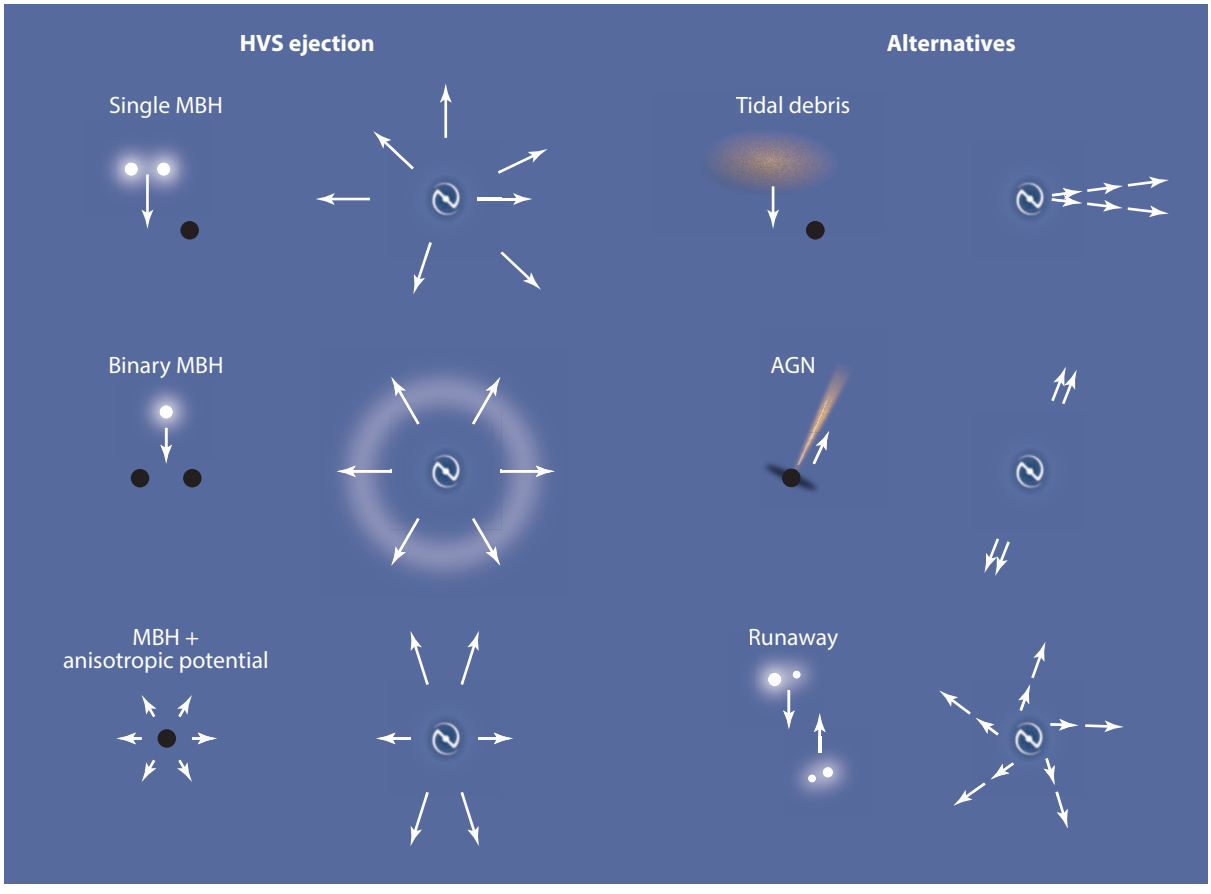

Figure 7

Diagram illustrating how different spatial distributions of hypervelocity stars (HVSs) link to different ejection mechanisms. Some mechanisms produce bursts, whereas others produce continuous ejections; most produce nonisotropic spatial distributions of unbound stars. Abbreviations: AGN, active galactic nucleus; MBH, massive black hole.

the potential, for example, HVSs should appear in two clumps on opposite sides of the sky with all possible flight times.

6.7.2. Observations. The HVS Survey provides a clean test of spatial distribution for a uniform set of unbound stars, complete over 29% of the sky. **Figure 8** plots the distribution of HVS Survey stars. Unbound stars in the HVS Survey are distributed equally across Galactic latitude. There is no statistical difference between the latitude distribution of the unbound stars and the underlying survey stars. A uniform latitude distribution is inconsistent with a disk runaway origin but consistent with an MBH origin.

However, the unbound stars in the HVS Survey are clumped in Galactic longitude (as seen in **Figure 8**). Specifically, 11 of the 21 unbound stars are located in a 25° × 25° region (5% of survey area) centered around (RA, Dec) = (167.5°, 3.0°) in the direction of the constellation Leo. The clump is statistically significant whether measured by longitude distribution, angular separation distribution, or the two-point angular correlation function (Brown et al. 2009b, 2012b).

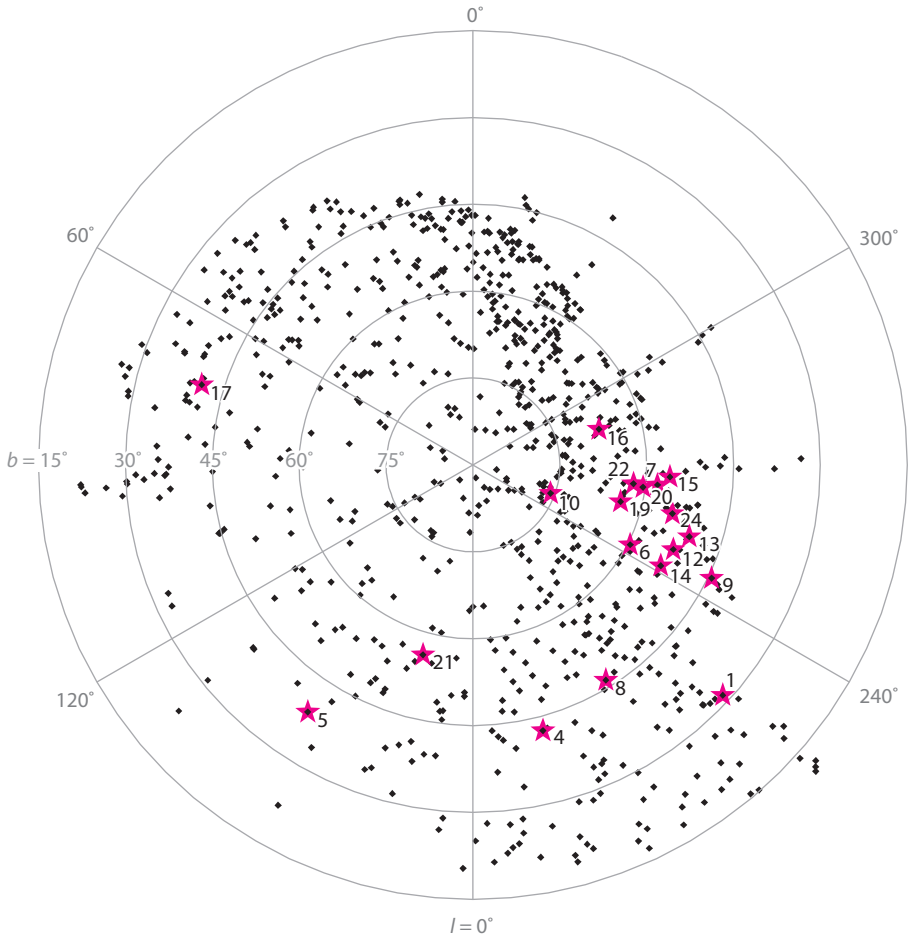

Figure 8

Polar projection, in Galactic coordinates, showing the spatial distribution of Hypervelocity Star (HVS) Survey stars with measured radial velocities. The overall distribution reflects the imaging footprint of the Sloan Digital Sky Survey. Unbound HVSs are marked by magenta stars. HVSs are found at all Galactic latitudes, but half are clumped around the constellation Leo. Adapted from Brown et al. (2014) with permission.

Unfortunately, the flight time uncertainties are too large to determine whether the clump of unbound stars share a common flight time (Brown et al. 2014).

At present, there is no good explanation for the anisotropic distribution of unbound late B-type stars in the halo. The tidal debris scenario is one possibility; however, it requires a gas-rich star-forming dwarf galaxy to account for the short-lived B stars, and no other tidal debris is observed. Interestingly, the unbound stars fall on the projected orbital planes of the clockwise and counter-clockwise disks of stars that now orbit Sgr A* (Lu et al. 2010, Zhang et al. 2013); however, there is no explanation for how these orbital planes remain fixed over the 200-Myr span of flight times. It is worth noting that the observed clump of unbound stars abuts the edge of the HVS Survey defined by the celestial equator. A full understanding of the spatial distribution requires a Southern Hemisphere survey.

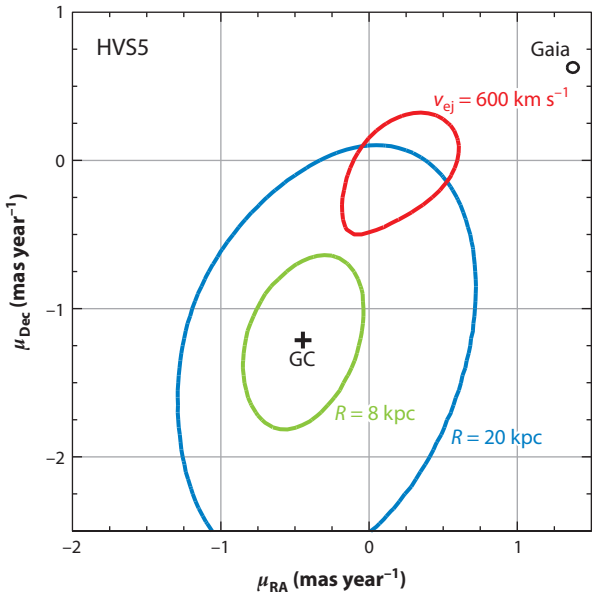

Figure 9

The proper motion of HVS5 ($v_{rf} = +650 \pm 4.3$ km s^{-1}, $R = 50 \pm 5$ kpc, $m_* = 3.6$ M$_\odot$) is not yet known. This figure illustrates how different trajectories map into proper motion space. Green and blue ellipses are the locus of HVS5 trajectories that pass within 8 and 20 kpc, respectively, of the Galactic Center (GC). The trajectory that passes through the GC is marked with a plus symbol (+). The locus of HVS5 trajectories with disk plane ejection velocities of 600 km s^{-1}, the escape velocity from the surface of the star, is drawn by the red contour. Physically allowed disk ejections are thus limited to the outer disk. The black circle is the size of the predicted *Gaia* proper motion measurement error, which will cleanly discriminate between outer disk and GC origins. Adapted from Brown et al. (2014) with permission.

6.8. Proper Motion

6.8.1. Background. Proper motion measurements promise to provide a direct constraint on the origin of HVSs. Proper motions, combined with distance and radial velocity, provide the full space trajectory of a star. Interestingly, a Galactic Center origin is often well separated in proper motion from a disk origin. This separation occurs because disk ejections are limited to those locations where the ejection velocity is less than the escape velocity from the surface of the star, $\simeq$600 km s^{-1}. For the fastest known HVSs, possible disk ejection locations are limited to the outer disk. **Figure 9** illustrates the case of HVS5 (Brown et al. 2012a).

Unfortunately, known HVSs are distant and on radial trajectories. Their expected proper motions are too small ($\leq$1 mas year^{-1}) to be measured with ground-based surveys. Proper motions with $<$0.1-mas year^{-1} uncertainties, like those promised by the *Gaia* mission (de Bruijne 2012), can provide a clean separation between Galactic disk and Galactic Center origins.

Proper motions accurate to $<$0.1 mas year^{-1} also open the door to identifying new stellar types of HVSs. Because HVSs have systematically larger velocities than other Galactic stars, they can be efficiently culled from large surveys using a combination of proper motion, radial velocity, and distance (Kenyon et al. 2014).

6.8.2. Observations. The first unbound star with a significant proper motion measurement is the hyper-runaway HD 271791 (Heber et al. 2008a). This star has nine proper motion measurements

with a root-mean-square scatter of 40%. The proper motion measurements show that HD 271791 was ejected from the outer disk in the direction of Galactic rotation, consistent with the hyper-runaway origin scenario. A Galactic Center origin is ruled out at the 3-σ level.

The proper motion of HE 0437−5439, the unbound star near the LMC, was measured with a pair of *Hubble Space Telescope* images. Its trajectory appears to come from the Milky Way; an origin from the center of the LMC is ruled out at the 3-σ level (Brown et al. 2010). To reconcile its main-sequence lifetime with its flight time from the Milky Way requires that HE 0437−5439 is a blue straggler. The required ejection velocity rules out runaway scenarios. Combining the observed trajectory, stellar nature, and ejection velocity, HE 0437−5439 was most likely a compact binary ejected by the Milky Way's central black hole (e.g., Perets 2009b). However, given the systematic uncertainty in the proper motion measurement, Irrgang et al. (2013) argue that an LMC origin is not ruled out. An LMC origin would be exciting evidence for an MBH in the LMC but requires an improved proper motion measurement.

The 20 nearby G- and K-type stars with possible unbound tangential velocities are identified by a single proper motion measurement (Palladino et al. 2014). The proper motions point to a disk origin, consistent with runaway origin scenarios.

The likely unbound 9-$M_\odot$ B star, LAMOST-HVS1, currently has two discrepant proper motion measurements. One measurement points from the outer disk; the other points from the Galactic Center (Zheng et al. 2014).

Proper motions exist for some of the unbound B stars in the HVS Survey, but the measurements have large uncertainties and are consistent with zero proper motion. The best that can be said is that the unbound B stars do not appear to come from other galaxies but likely have proper motions compatible with radial trajectories from the Milky Way.

Overall, existing proper motions suffer large uncertainties and poorly constrain the origin of unbound stars. The most significant constraints are for special cases in which the origin can be easily distinguished between two alternatives. In all cases, more accurate measurements are needed.

6.9. Galactic Center Observations

Galactic Center observations provide additional constraints on the origin of HVSs. The Hills mechanism requires that the former companion of an HVS is left behind in a tightly bound orbit around the MBH. The nature, number, and distribution of the S stars around the central MBH are remarkably consistent with expectations for the former companions of HVSs.

6.9.1. Stellar nature of the S stars. Adaptive optics–assisted spectroscopy of the stars in the central arcsec of the Galaxy establish that the S stars are normal main-sequence B stars (Ghez et al. 2003, Eisenhauer et al. 2005). Yet the tidal forces of the MBH are too strong to permit star formation in the central arcsec (Morris 1993). The short-lived B stars next to the MBH must therefore form elsewhere and then migrate to their current location.

A viable explanation for this "paradox of youth" is that the S stars are captured by the MBH in a 3-body exchange scenario (Gould & Quillen 2003). Alternative explanations, such as making B-type-looking stars through the tidal stripping of old red giants (Davies & King 2005), have been ruled out by detailed observations (Martins et al. 2008). Alternative mechanisms for capturing stars next to the MBH, e.g., the in-spiral of a massive young star cluster, are ruled out by the available timescales and the observed density profile of stars in the Galactic Center (Perets & Gualandris 2010). The Hills mechanism, by contrast, successfully explains the B stars in close orbit around the MBH.

6.9.2. Number of S stars. The number of S stars in the central arcsec is consistent with the Hills mechanism. As previously mentioned, S star orbits are predicted to evolve dynamically, and some objects will suffer tidal disruption before reaching the end of their lives (e.g., Perets et al. 2009a). When these effects are accounted for, the observed number of S stars implies a capture rate of 2×10^{-7} year^{-1} for stars with masses exceeding 5 $M_\odot$ (Bromley et al. 2012). For a Salpeter mass function, this capture rate matches the ejection rate of unbound 2.5–4 $M_\odot$ stars in the HVS Survey (Kenyon et al. 2014). Thus the number of unbound B-type stars in the halo appears consistent with the number of B-type stars orbiting the central MBH.

6.9.3. Orbital distribution of S stars. The orbital distribution of S stars provides additional constraint on their origin. The S stars are observed to have randomly oriented orbits and a thermal distribution of eccentricities (Gillessen et al. 2009). This distribution is consistent with the Hills mechanism (Perets et al. 2009a, Zhang et al. 2013, Madigan et al. 2014).

S stars captured via the Hills binary disruption scenario begin with highly eccentric orbits. The highly eccentric orbits then evolve dynamically owing to gravitational perturbations. The timescale for evolution depends on assumptions about whether binaries come from a stellar disk or from further out by massive perturbers, and the presence of a cusp (Perets & Gualandris 2010, Madigan et al. 2011, Antonini & Merritt 2013, Zhang et al. 2013). Models with a cusp of 1,000 SBHs can successfully evolve the orbits of binaries into the observed S star eccentricity distribution (Antonini 2014). Alternatively, if the stellar disk was once more massive and extended closer to the MBH, a rapidly evolving region inside the central arcsecond could successfully redistribute stars from the disk into the observed S star distribution (Chen & Amaro-Seoane 2014).

A second constraint arises from the orbital distribution of stars captured at larger radii and onto longer period orbits. Stars at larger radii should retain their original eccentricities because 2-body and resonant relaxation timescales are long (Perets & Gualandris 2010). To observe this effect requires measuring the orbital motions of longer-lived, and thus fainter, stars in the Galactic Center. Remarkably, recent observations find that the faintest, late B-type stars have systematically more radial orbits at larger radii from the MBH, exactly as expected for the Hills binary disruption origin scenario (Madigan et al. 2014).

6.10. Summary of Observations

HVSs are stars ejected at unbound speeds by the Milky Way's MBH. The Milky Way's MBH must eject HVSs, and the unbound stars that are observed in the halo support the MBH ejection origin. The supporting observations include the velocities of the unbound stars, velocities that in certain cases exceed the escape velocity from the surface of the stars. The velocity distribution of both unbound and bound stars in the HVS Survey is consistent with predicted HVS ejection velocity distributions. The unbound B stars are, on the basis of their rotation, main-sequence stars and must originate from a region of ongoing star formation like the Galactic Center. The observed number of unbound B stars is consistent with theoretically predicted HVS ejection rates but inconsistent with hyper-runaway ejection rates. The distribution in Galactic latitude of unbound B stars is consistent with Galactic Center ejections but inconsistent with disk ejections. The four brightest HVSs in the HVS Survey were ejected 100 Myr after they were formed, which is a timescale consistent with a Galactic Center origin but inconsistent with scenarios that require a prompt ejection as in the runaway or AGN scenarios. Finally, the nature, number, and orbital distribution of S stars orbiting the MBH in the central arcsecond of the Galaxy are consistent with their being the former companions of HVSs. Other observations, such as the distribution

of $v \sin i$, flight time, metallicity, and proper motion of unbound B stars, currently provide no significant constraint on origin but can be further improved. Taken together, the current set of observations is consistent with an MBH origin for unbound HVSs.

7. FUTURE PROSPECTS

7.1. Links to Dark Matter

HVSs are potentially important tools to probe a variety of phenomena not limited to MBHs. An especially interesting application is the use of HVSs as test particles to map the Galaxy's matter and dark matter distribution. Launched from the center of the Galaxy, HVSs integrate the Galactic potential as they travel to >100-kpc distances. Because many HVSs are observed traveling near Galactic escape velocity, both their speeds and their trajectories provide unique constraints on the Galaxy's mass distribution (Gnedin et al. 2005).

The three-dimensional motions of HVSs constrain the shape and orientation of the Galaxy's mass distribution (Gnedin et al. 2005, Yu & Madau 2007). A generic prediction of hierarchical, cold dark matter models is that galaxies have triaxial dark matter distributions. HVSs are launched on radial trajectories. If the Galactic potential is triaxial, the present motion of HVSs must deviate from being precisely radial. To measure any nonradial motion requires accurate proper motions and distances, which is difficult. Distance errors can be mitigated by using HVSs in different directions on the sky. With a sufficient number of HVSs, it should be possible to measure the two axis ratios and three direction angles of the triaxial halo, independent of any other technique (Gnedin et al. 2005).

The asymmetry in the velocity distribution of outgoing versus incoming stars provides a different, empirical measure of escape velocity over distance, regardless of the underlying distribution of HVS ejection velocity. Unbound HVSs are, by definition, only observed on outgoing trajectories; HVSs launched on bound orbits fill phase space over time. Different Galactic potential models give different orbital return times. If the stellar nature of the HVSs is known and if HVS ejections are continuous, then the ratio of outgoing to incoming stars can constrain the Galactic potential (Kenyon et al. 2008, Perets et al. 2009b).

7.2. Links to Black Hole Growth, Supernovae, and Cosmology

HVSs are directly linked to tidal disruption events and the growth of central MBHs. Every HVS ejected by the Hills mechanism leaves its former companion behind, orbiting the MBH. Dynamical calculations suggest that a significant fraction of the former companions produce tidal disruption events (Bromley et al. 2012). Given the observed numbers of HVSs and S stars in the Milky Way, the central MBH may have grown by a factor of 2–4 in the past 5–10 Gyr simply owing to binary disruptions and subsequent tidal disruption events. The ejection rate of HVSs is thus linked to the mass growth of central MBHs (Bromley et al. 2012).

The relationship between HVSs and hostless supernovae is more speculative. Because of their large velocities, HVSs inevitably evolve and die far from where they form. However, HVSs are a rare population, and massive stars responsible for core-collapse supernovae are only 1% of a Kroupa mass function by number. The ejection rate of HVSs that explode as (hostless) Type II supernovae is thus $\sim 10^{-6}$ year^{-1} for the Milky Way. This rate is 10,000 times lower than the rate of normal Type II supernovae in the Milky Way (Li et al. 2011). To find an HVS supernova requires observing ~10,000 normal Type II supernovae. In a present sample of 600

Type II core-collapse supernovae, there is only one possible HVS supernova candidate that has a projected distance of >10 kpc from its nearest galaxy with no possibility of a closer low surface brightness galaxy (Zinn et al. 2011). Future surveys, such as with the Large Synoptic Survey Telescope, may be able to identify an HVS supernova.

Long-lived HVSs travel the distance between galaxies within a Hubble time. For example, HVSs ejected from M31 reach the Milky Way in approximately 1 Gyr. Theoretical calculations show that HVSs originating from M31 are gravitationally focused by the Milky Way and should have a local density of 10^{-3} kpc^{-3} (Sherwin et al. 2008). To find one M31 HVS near the Sun thus requires surveying a 1,000-kpc^3 volume. Unfortunately, long-lived HVSs are intrinsically faint stars and difficult to distinguish from other stars commonly found in the Milky Way.

Unrelated to HVSs in the Milky Way, the globular cluster traveling −1,025 km s^{-1} near M87 in the Virgo Cluster may share a similar origin. The cluster is dubbed a hypervelocity globular cluster because a 3-body interaction with M87's MBH is one possible explanation for its extreme velocity (Caldwell et al. 2014).

In the distant future, HVSs may become tools for cosmology. When the Universe has aged by a factor of ten in the standard cosmological model, the only extragalactic sources of light in the observable cosmic volume will be HVSs ejected from our Galaxy. Thus HVSs may become the primary tool for measuring the Hubble expansion (Loeb 2011). For now, HVSs are important tools for probing the nature and environment of MBHs and for mapping the shape of the Milky Way dark matter halo.

7.3. Next Steps

To distinguish among the various proposed HVS ejection mechanisms, future imaging and proper motion surveys are needed to obtain larger samples of HVSs. A sample of 50–100 HVSs is required, for example, to cleanly discriminate ejection mechanisms on the basis of ejection velocity distribution (Sesana et al. 2007, Perets 2009b). Different ejection mechanisms also predict different spatial distributions of HVSs (Levin 2006, Abadi et al. 2009, Zhang et al. 2013). Because only a third of the sky imaged by the SDSS has been systematically searched for HVSs, a survey of the southern sky will enable improved constraints on the origin of HVSs.

Multipassband imaging surveys with the SkyMapper telescope (Keller et al. 2007), the VLT Survey Telescope, and the future Large Synoptic Survey Telescope will enable the first systematic searches for HVSs in the Southern Hemisphere. Having *u*-band photometry is particularly important for HVS target selection, because the strongest surface gravity- and metallicity-sensitive spectral features are in the blue for all stars hotter than solar-type stars. Simply applying the HVS Survey color selection to SkyMapper should, for example, double the number of unbound B-type HVSs. This is important because the angular distribution of a uniform sample of HVSs over the entire sky, as well as their distribution of flight times, can discriminate among different proposed HVS ejection mechanisms (see Sections 6.4 and 6.7).

The *Gaia* space astrometry mission will open the door to finding a variety of nearby <10-kpc HVSs through a combination of proper motion, distance, and radial velocity measurements (Kenyon et al. 2014). For known HVSs, *Gaia*'s expected 0.01–0.1-mas year^{-1} proper motion accuracies will place direct constraints on HVS origin (Brown et al. 2014). Accurate proper motions are also the key for using HVSs to trace out the Milky Way's gravitational potential.

We are at an exciting time in the study of HVSs. New HVS candidates will soon come from Southern Hemisphere imaging surveys. The distribution of HVSs in large, uniform surveys will test proposed HVS ejection mechanisms. *Gaia* proper motions may directly link HVSs to their MBH origin. The future of HVSs appears unbounded.

SUMMARY POINTS

1. Unbound HVSs are a natural consequence of the multiplicity of stars and the existence of MBHs (Hills 1988).
2. HVSs are ejected from all galaxies with an MBH, but only those ejected from the Milky Way can currently be observed.
3. The first observed HVS is an unbound 3-$M_\odot$ star 100 kpc from the Sun traveling with a velocity of at least 673 km s^{-1}, a speed in excess of the escape velocity from the surface of the star (Brown et al. 2005).
4. Different MBH ejection mechanisms, such as a single or binary MBH, predict different velocity and spatial distributions of HVSs.
5. The velocities, stellar nature, arrival times, angular positions, and overall number of unbound B stars in the Milky Way halo, as well as the S stars around the MBH, support the MBH ejection origin. Alternative origins are inconsistent with the full set of observations.
6. In the future, Southern Hemisphere samples will map the all-sky distribution of HVSs and discriminate among MBH ejection scenarios. Proper motions measurements will provide more direct links to the MBH. If HVSs are indeed ejected from the Galactic Center, then their 3D trajectories may provide unique constraints on the distribution of dark matter surrounding the Milky Way.

DISCLOSURE STATEMENT

The author is not aware of any affiliations, memberships, funding, or financial holdings that might be perceived as affecting the objectivity of this review.

ACKNOWLEDGMENTS

I thank Margaret Geller, Scott Kenyon, and Charles King III for their support and helpful comments. This work was supported in part by National Science Foundation grant no. PHYS-1066293 and the hospitality of the Aspen Center for Physics. This work was also supported by the Smithsonian Institution.

LITERATURE CITED

Abadi MG, Navarro JF, Steinmetz M. 2009. *Ap. J. Lett.* 691:L63–66
Abt HA, Levato H, Grosso M. 2002. *Ap. J.* 573:359–65
Antonini F. 2014. *Ap. J.* 749:106
Antonini F, Faber J, Gualandris A, Merritt D. 2010. *Ap. J.* 713:90–104
Antonini F, Lombardi JC Jr, Merritt D. 2011. *Ap. J.* 731:128
Antonini F, Merritt D. 2013. *Ap. J. Lett.* 763:L10
Bahcall JN, Wolf RA. 1976. *Ap. J.* 209:214–32
Bailey JD, Landstreet JD, Bagnulo S. 2014. *Astron. Astrophys.* 561:A147
Bartko H, Martins F, Fritz TK, et al. 2009. *Ap. J.* 697:1741–63
Bartko H, Martins F, Trippe S, et al. 2010. *Ap. J.* 708:834–40
Baruteau C, Cuadra J, Lin DNC. 2011. *Ap. J.* 726:28
Baumgardt H, Gualandris A, Portegies Zwart S. 2006. *MNRAS* 372:174–82

Behr BB. 2003a. *Ap. J. Suppl. Ser.* 149:67–99
Behr BB. 2003b. *Ap. J. Suppl. Ser.* 149:101–21
Blaauw A. 1961. *Bull. Astron. Inst. Neth.* 15:265
Bonanos AZ, López-Morales M, Hunter I, Ryans RSI. 2008. *Ap. J. Lett.* 675:L77–80
Bovy J, Rix HW. 2013. *Ap. J.* 779:115
Bromley BC, Brown WR, Geller MJ, Kenyon SJ. 2009. *Ap. J.* 706:925–40
Bromley BC, Kenyon SJ, Geller MJ, Brown WR. 2012. *Ap. J. Lett.* 749:L42
Bromley BC, Kenyon SJ, Geller MJ, et al. 2006. *Ap. J.* 653:1194–202
Brown WR, Anderson J, Gnedin OY, et al. 2010. *Ap. J. Lett.* 719:L23–27
Brown WR, Cohen JG, Geller MJ, Kenyon SJ. 2012a. *Ap. J. Lett.* 754:L2
Brown WR, Cohen JG, Geller MJ, Kenyon SJ. 2013. *Ap. J.* 775:32
Brown WR, Geller MJ, Kenyon SJ. 2009a. *Ap. J.* 690:1639–47
Brown WR, Geller MJ, Kenyon SJ. 2012b. *Ap. J.* 751:55
Brown WR, Geller MJ, Kenyon SJ. 2014. *Ap. J.* 787:89
Brown WR, Geller MJ, Kenyon SJ, Bromley BC. 2009b. *Ap. J. Lett.* 690:L69–71
Brown WR, Geller MJ, Kenyon SJ, Kurtz MJ. 2005. *Ap. J. Lett.* 622:L33–36
Brown WR, Geller MJ, Kenyon SJ, Kurtz MJ. 2006a. *Ap. J. Lett.* 640:L35
Brown WR, Geller MJ, Kenyon SJ, Kurtz MJ. 2006b. *Ap. J.* 647:303
Brown WR, Geller MJ, Kenyon SJ, Kurtz MJ, Bromley BC. 2007a. *Ap. J.* 660:311
Brown WR, Geller MJ, Kenyon SJ, Kurtz MJ, Bromley BC. 2007b. *Ap. J.* 671:1708
Buchholz RM, Schödel R, Eckart A. 2009. *Astron. Astrophys.* 499:483–501
Caldwell N, Strader J, Romanowsky AJ, et al. 2014. *Ap. J. Lett.* 787:L11
Carr JS, Sellgren K, Balachandran SC. 2000. *Ap. J.* 530:307–22
Chatterjee S, Vlemmings WHT, Brisken WF, et al. 2005. *Ap. J. Lett.* 630:L61–64
Chen X, Amaro-Seoane P. 2014. *Ap. J. Lett.* 786:L14
Chini R, Hoffmeister VH, Nasseri A, Stahl O, Zinnecker H. 2012. *MNRAS* 424:1925–29
Christopher MH, Scoville NZ, Stolovy SR, Yun MS. 2005. *Ap. J.* 622:346–65
Davies MB, King A. 2005. *Ap. J. Lett.* 624:L25–27
de Bruijne JHJ. 2012. *Ap. Space Sci.* 341:31–41
de Mink SE, Sana H, Langer N, Izzard RG, Schneider FRN. 2014. *Ap. J.* 782:7
De Rosa RJ, Patience J, Wilson PA, et al. 2014. *MNRAS* 437:1216–40
Deason AJ, Belokurov V, Koposov SE, Rockosi CM. 2014. *Ap. J.* 787:30
Do T, Ghez AM, Morris MR, et al. 2009. *Ap. J.* 703:1323–37
Do T, Martinez GD, Yelda S, et al. 2013. *Ap. J. Lett.* 779:L6
Donley JL, Brandt WN, Eracleous M, Boller T. 2002. *Astron. J.* 124:1308–21
Duchêne G, Kraus A. 2013. *Annu. Rev. Astron. Astrophys.* 51:269–310
Edelmann H, Napiwotzki R, Heber U, Christlieb N, Reimers D. 2005. *Ap. J. Lett.* 634:L181–84
Eisenhauer F, Genzel R, Alexander T, et al. 2005. *Ap. J.* 628:246–59
Figer DF, Kim SS, Morris M, et al. 1999. *Ap. J.* 525:750–58
Fregeau JM, Cheung P, Portegies Zwart SF, Rasio FA. 2004. *MNRAS* 352:1–19
Fuentes CI, Stanek KZ, Gaudi BS, et al. 2006. *Ap. J. Lett.* 636:L37–40
Fuhrmann K, Chini R. 2012. *Ap. J. Suppl. Ser.* 203:30
Gebran M, Vick M, Monier R, Fossati L. 2010. *Astron. Astrophys.* 523:A71
Geier S, Marsh TR, Wang B, et al. 2013. *Astron. Astrophys.* 554:A54
Gerhard O. 2001. *Ap. J. Lett.* 546:L39–42
Gezari S, Heckman T, Cenko SB, et al. 2009. *Ap. J.* 698:1367–79
Ghez AM, Duchêne G, Matthews K, et al. 2003. *Ap. J. Lett.* 586:L127–31
Ghez AM, Salim S, Hornstein SD, et al. 2005. *Ap. J.* 620:744
Ghez AM, Salim S, Weinberg NN, et al. 2008. *Ap. J.* 689:1044–62
Gies DR, Bolton CT. 1986. *Ap. J. Suppl. Ser.* 61:419–54
Gillessen S, Eisenhauer F, Trippe S, et al. 2009. *Ap. J.* 692:1075–109
Ginsburg I, Loeb A. 2006. *MNRAS* 368:221–25
Ginsburg I, Loeb A. 2007. *MNRAS* 376:492–96

Girardi L, Grebel EK, Odenkirchen M, Chiosi C. 2004. *Astron. Astrophys.* 422:205–15
Gnedin OY, Gould A, Miralda-Escudé J, Zentner AR. 2005. *Ap. J.* 634:344–50
Gould A, Quillen AC. 2003. *Ap. J.* 592:935–40
Greenstein JL, Sargent AI. 1974. *Ap. J. Suppl. Ser.* 28:157
Gualandris A, Merritt D. 2009. *Ap. J.* 705:361–71
Gualandris A, Portegies Zwart S. 2007. *MNRAS* 376:L29–33
Gualandris A, Portegies Zwart S, Sipior MS. 2005. *MNRAS* 363:223–28
Guesten R, Genzel R, Wright MCH, et al. 1987. *Ap. J.* 318:124–38
Gvaramadze VV, Gualandris A. 2011. *MNRAS* 410:304–12
Gvaramadze VV, Gualandris A, Portegies Zwart S. 2009. *MNRAS* 396:570–78
Hansen BMS. 2007. *Ap. J. Lett.* 671:L133–36
Hansen BMS, Milosavljević M. 2003. *Ap. J. Lett.* 593:L77–80
Hansen BMS, Phinney ES. 1997. *MNRAS* 291:569
Hayden MR, Holtzman JA, Bovy J, et al. 2014. *Astron. J.* 147:116
Heber U, Edelmann H, Napiwotzki R, Altmann M, Scholz RD. 2008a. *Astron. Astrophys.* 483:L21–24
Heber U, Hirsch HA, Edelmann H, et al. 2008b. In *Hot Subdwarf Stars and Related Objects*, ed. U Heber, CS Jeffery, R Napiwotzki, p. 167. *ASP Conf. Ser.* 392. Orem, UT: ASP
Hills JG. 1975. *Nature* 254:295–98
Hills JG. 1988. *Nature* 331:687–89
Hills JG. 1991. *Astron. J.* 102:704–15
Hills JG. 1992. *Astron. J.* 103:1955–69
Hirsch HA, Heber U, O'Toole SJ, Bresolin F. 2005. *Astron. Astrophys.* 444:L61–64
Hoogerwerf R, de Bruijne JHJ, de Zeeuw PT. 2001. *Astron. Astrophys.* 365:49–77
Hopkins PF. 2014. *MNRAS* 797:59
Hopman C. 2009. *Ap. J.* 700:1933–51
Huang W, Gies DR. 2006. *Ap. J.* 648:580–90
Humason ML, Zwicky F. 1947. *Ap. J.* 105:85
Irrgang A, Przybilla N, Heber U, Nieva MF, Schuh S. 2010. *Ap. J.* 711:138–43
Irrgang A, Wilcox B, Tucker E, Schiefelbein L. 2013. *Astron. Astrophys.* 549:A137
Justham S, Wolf C, Podsiadlowski P, Han Z. 2009. *Astron. Astrophys.* 493:1081–91
Karas V, Subr L. 2007. *Astron. Astrophys.* 470:11–19
Keller SC, Schmidt BP, Bessell MS, et al. 2007. *Proc. Astron. Soc. Aust.* 24:1–12
Kenyon SJ, Bromley BC, Brown WR, Geller MJ. 2014. *Ap. J.* 793:122
Kenyon SJ, Bromley BC, Geller MJ, Brown WR. 2008. *Ap. J.* 680:312–27
Kobayashi S, Hainick Y, Sari R, Rossi EM. 2012. *Ap. J.* 748:105
Kollmeier JA, Gould A. 2007. *Ap. J.* 664:343–48
Kollmeier JA, Gould A, Knapp G, Beers TC. 2009. *Ap. J.* 697:1543–48
Kollmeier JA, Gould A, Rockosi C, et al. 2010. *Ap. J.* 723:812–17
Kormendy J, Ho LC. 2013. *Annu. Rev. Astron. Astrophys.* 51:511–653
Kormendy J, Richstone D. 1995. *Annu. Rev. Astron. Astrophys.* 33:581
Kunder A, Koch A, Rich RM, et al. 2012. *Astron. J.* 143:57
Leigh NWC, Geller AM. 2013. *MNRAS* 432:2474–79
Leonard PJT. 1991. *Astron. J.* 101:562–71
Levin Y. 2006. *Ap. J.* 653:1203–9
Levin Y. 2007. *MNRAS* 374:515–24
Levin Y, Beloborodov AM. 2003. *Ap. J. Lett.* 590:L33–36
Li W, Chornock R, Leaman J, et al. 2011. *MNRAS* 412:1473–507
Li Y, Luo A, Zhao G, et al. 2012. *Ap. J. Lett.* 744:L24
Löckmann U, Baumgardt H. 2008. *MNRAS* 384:323–30
Löckmann U, Baumgardt H, Kroupa P. 2009. *MNRAS* 398:429–37
Loeb A. 2011. *J. Cosmol. Astropart. Phys.* 4:23
López-Morales M, Bonanos AZ. 2008. *Ap. J. Lett.* 685:L47–50
Lu JR, Do T, Ghez AM, et al. 2013. *Ap. J.* 764:155

Lu JR, Ghez AM, Hornstein SD, et al. 2009. *Ap. J.* 690:1463–87
Lu Y, Yu Q, Lin DNC. 2007. *Ap. J. Lett.* 666:L89–92
Lu Y, Zhang F, Yu Q. 2010. *Ap. J.* 709:1356–61
Madigan AM, Hopman C, Levin Y. 2011. *Ap. J.* 738:99
Madigan AM, Levin Y, Hopman C. 2009. *Ap. J. Lett.* 697:L44–48
Madigan AM, Pfuhl O, Levin Y, et al. 2014. *Ap. J.* 784:23
Martin JC. 2004. *Astron. J.* 128:2474–500
Martin JC. 2006. *Astron. J.* 131:3047–68
Martins F, Gillessen S, Eisenhauer F, et al. 2008. *Ap. J. Lett.* 672:L119–22
McAuley P. 1994. *Eternal Light.* London: Gollancz
McConnachie AW. 2012. *Astron. J.* 144:4
McKee CF, Ostriker EC. 2007. *Annu. Rev. Astron. Astrophys.* 45:565–687
Merritt D. 2013. *Dynamics and Evolution of Galactic Nuclei*. Princeton, NJ: Princeton Univ. Press
Merritt D, Gualandris A, Mikkola S. 2009. *Ap. J. Lett.* 693:L35–38
Merritt D, Poon MY. 2004. *Ap. J.* 606:788–98
Michaud G. 1970. *Ap. J.* 160:641
Miller MC, Freitag M, Hamilton DP, Lauburg VM. 2005. *Ap. J. Lett.* 631:L117–20
Morris M. 1993. *Ap. J.* 408:496–506
Muno MP, Pfahl E, Baganoff FK, et al. 2005. *Ap. J. Lett.* 622:L113–16
Nayakshin S. 2006. *MNRAS* 372:143–50
Nayakshin S, Sunyaev R. 2005. *MNRAS* 364:L23–27
Nieva MF, Przybilla N. 2012. *Astron. Astrophys.* 539:A143
O'Leary RM, Loeb A. 2008. *MNRAS* 383:86–92
Ott T, Eckart A, Genzel R. 1999. *Ap. J.* 523:248–64
Palladino LE, Schlesinger KJ, Holley-Bockelmann K, et al. 2014. *Ap. J.* 780:7
Perlman D. 2005. Wandering star screaming from Milky Way/runaway youngster clocked at more than 1.5 million mph. *San Francisco Chronicle*, Feb. 11
Pereira CB, Jilinski E, Drake NA, et al. 2012. *Astron. Astrophys.* 543:A58
Pereira CB, Jilinski EG, Drake NA, Ortega VG, Roig F. 2013. *Astron. Astrophys.* 559:A12
Perets HB. 2009a. *Ap. J.* 690:795–801
Perets HB. 2009b. *Ap. J.* 698:1330–40
Perets HB, Gualandris A. 2010. *Ap. J.* 719:220–28
Perets HB, Gualandris A, Kupi G, Merritt D, Alexander T. 2009a. *Ap. J.* 702:884–89
Perets HB, Hopman C, Alexander T. 2007. *Ap. J.* 656:709–20
Perets HB, Subr L. 2012. *Ap. J.* 751:133
Perets HB, Wu X, Zhao HS, et al. 2009b. *Ap. J.* 697:2096–101
Pflamm-Altenburg J, Kroupa P. 2010. *MNRAS* 404:1564–68
Pfuhl O, Alexander T, Gillessen S, et al. 2014. *Ap. J.* 782:101
Pfuhl O, Fritz TK, Zilka M, et al. 2011. *Ap. J.* 741:108
Piffl T, Scannapieco C, Binney J, et al. 2014. *Astron. Astrophys.* 562:A91
Piffl T, Williams M, Steinmetz M. 2011. *Astron. Astrophys.* 535:A70
Porcel C, Garzon F, Jimenez-Vicente J, Battaner E. 1998. *Astron. Astrophys.* 330:136–38
Portegies Zwart SF. 2000. *Ap. J.* 544:437–42
Portegies Zwart SF, Baumgardt H, McMillan SLW, et al. 2006. *Ap. J.* 641:319–26
Poveda A, Ruiz J, Allen C. 1967. *Bol. Obs. Tonantzintla Tacubaya* 4:860
Przybilla N, Nieva MF, Heber U, Butler K. 2008a. *Ap. J. Lett.* 684:L103–6
Przybilla N, Nieva MF, Heber U, et al. 2008b. *Astron. Astrophys.* 480:L37–40
Przybilla N, Nieva MF, Tillich A, et al. 2008c. *Astron. Astrophys.* 488:L51–54
Ramírez SV, Sellgren K, Carr JS, et al. 2000. *Ap. J.* 537:205–20
Rauch KP, Tremaine S. 1996. *New Astron.* 1:149–70
Reid MJ, Brunthaler A. 2004. *Ap. J.* 616:872–84
Reid MJ, Menten KM, Brunthaler A, et al. 2014. *Ap. J.* 783:130
Robitaille TP, Whitney BA. 2010. *Ap. J. Lett.* 710:L11–15

Rossi EM, Kobayashi S, Sari R. 2014. *Ap. J.* 795:125
Ryde N, Schultheis M. 2015. *Astron. Astrophys.* 573:A14
Sana H, de Mink SE, de Koter A, et al. 2012. *Science* 337:444
Schodel R, Feldmeier A, Kunneriath D, et al. 2014. *Astron. Astrophys.* 566:A47
Sesana A, Haardt F, Madau P. 2006. *Ap. J.* 651:392–400
Sesana A, Haardt F, Madau P. 2007. *MNRAS* 379:L45–49
Sesana A, Haardt F, Madau P. 2008. *Ap. J.* 686:432–47
Sesana A, Madau P, Haardt F. 2009. *MNRAS* 392:L31–34
Sherwin BD, Loeb A, O'Leary RM. 2008. *MNRAS* 386:1179–91
Silk J, Antonuccio-Delogu V, Dubois Y, et al. 2012. *Astron. Astrophys.* 545:L11
Silva MDV, Napiwotzki R. 2011. *MNRAS* 411:2596–614
Sirko E, Goodman J, Knapp GR, et al. 2004. *Astron. J.* 127:899–913
Smith MC, Ruchti GR, Helmi A, et al. 2007. *MNRAS* 379:755–72
Stolte A, Ghez AM, Morris M, et al. 2008. *Ap. J.* 675:1278–92
Stone RC. 1991. *Astron. J.* 102:333–49
Tillich A, Heber U, Geier S, et al. 2011. *Astron. Astrophys.* 527:A137
Tillich A, Przybilla N, Scholz R, Heber U. 2009. *Astron. Astrophys.* 507:L37–40
Tokovinin A. 2014. *Astron. J.* 147:87
Turner DG, Kovtyukh VV, Majaess DJ, Lane DJ, Moncrieff KE. 2009. *Astron. Nachr.* 330:807
Tutukov AV, Fedorova AV. 2009. *Astron. Rep.* 53:839–49
van Velzen S, Farrar GR. 2014. *Ap. J.* 792:53
Wang B, Han Z. 2009. *Astron. Astrophys.* 508:L27–30
Wang B, Justham S, Han Z. 2013. *Astron. Astrophys.* 559:A94
Wang J, Merritt D. 2004. *Ap. J.* 600:149–61
Weidner C, Kroupa P. 2006. *MNRAS* 365:1333–47
Xue XX, Rix HW, Yanny B, et al. 2011. *Ap. J.* 738:79
Yanny B, Rockosi C, Newberg HJ, et al. 2009. *Astron. J.* 137:4377–99
Yelda S, Ghez AM, Lu JR, et al. 2014. *Ap. J.* 783:131
Yu Q, Madau P. 2007. *MNRAS* 379:1293–301
Yu Q, Tremaine S. 2003. *Ap. J.* 599:1129–38
Zhang F, Lu Y, Yu Q. 2010. *Ap. J.* 722:1744–61
Zhang F, Lu Y, Yu Q. 2013. *Ap. J.* 768:153
Zheng Z, Carlin JL, Beers TC, et al. 2014. *Ap. J. Lett.* 785:L23
Zhong J, Chen L, Liu C, et al. 2014. *Ap. J. Lett.* 789:L2
Zinn PC, Grunden P, Bomans DJ. 2011. *Astron. Astrophys.* 536:A103
Zubovas K, Nayakshin S, Sazonov S, Sunyaev R. 2013. *MNRAS* 431:793–98

Annual Review of Astronomy and Astrophysics

Volume 53, 2015

Contents

Indexes

Errata

An online log of corrections to *Annual Review of Astronomy and Astrophysics* articles may be found at http://www.annualreviews.org/errata/astro